



Historical Perspective

## Protein-based polyelectrolyte multilayers

Aurélien vander Straeten<sup>\*</sup>, Damien Lefèvre, Sophie Demoustier-Champagne, Christine Dupont-Gillain

*Institute of Condensed Matter and Nanosciences, Université catholique de Louvain, Place Louis Pasteur, 1 bte L4.01.10, B-1348 Louvain-la-Neuve, Belgium*

### ARTICLE INFO

#### Article history:

13 April 2020

Available online 19 April 2020

#### Keywords:

Layer-by-layer

Protein

Polyelectrolyte

Biomaterial

Multilayer

Biosensing

Drug delivery

### ABSTRACT

The immobilization of proteins to impart specific functions to surfaces is topical for chemical engineering, healthcare and diagnosis. Layer-by-Layer (LbL) self-assembly is one of the most used method to immobilize macromolecules on surfaces. It consists in the alternate adsorption of oppositely charged species, resulting in the formation of a multilayer. This method in principle allows any charged object to be immobilized on any surface, from aqueous solutions. However, when it comes to proteins, the promises of versatility, simplicity and universality that the LbL approach holds are unmet due to the heterogeneity of protein properties. In this review, the literature is analyzed to make a generic approach emerge, with a view to facilitate the LbL assembly of proteins with polyelectrolytes (PEs). In particular, this review aims at guiding the choice of the PE and the building conditions that lead to the successful growth of protein-based multilayered self-assemblies.

© 2020 Elsevier B.V. All rights reserved.

### Contents

1. Introduction . . . . .	1
2. Strategies for the successful LbL assembly of protein with polyelectrolyte . . . . .	6
3. Intrinsic and extrinsic parameters: Impact on the growth of protein-based multilayer films . . . . .	7
3.1. Extrinsic parameters . . . . .	7
3.1.1. pH of the solution . . . . .	7
3.1.2. Presence of salts in solution. . . . .	10
3.1.3. Temperature . . . . .	11
3.1.4. Concentration of the protein solution . . . . .	12
3.2. Intrinsic parameters . . . . .	12
3.2.1. Nature of the PE . . . . .	12
3.2.2. Nature of the protein. . . . .	13
3.2.3. Supporting material . . . . .	13
4. Protein bioactivity in the LbL assembly . . . . .	13
5. Protein crystals and protein-PE complexes as building blocks for assembly . . . . .	14
6. Conclusions and future prospects. . . . .	15
Author contributions. . . . .	16
Acknowledgment . . . . .	16
References . . . . .	16

### 1. Introduction

Functional materials are the basis of a wide range of technologies. Whether these materials are created for medical applications, sensing, energy storage and generation or chemical transformation, they all share the common feature that their performance is dictated by their

ability to interact with the surrounding environment. The easiest way to control materials functionalities is thus through engineering of their surfaces. Therefore, surface modification and coating technologies have become prevalent and a vast array of methods were developed over the last century. Each surface modification technique offers advantages and drawbacks. Yet the perfect coating should, on top of offering the desired functionalities, be constructed easily and in mild conditions, and be versatile towards the surface geometry and chemistry.

<sup>\*</sup> Corresponding author.

E-mail address: [aurelien.vanderstraeten@uclouvain.be](mailto:aurelien.vanderstraeten@uclouvain.be) (A. vander Straeten).

In this view, self-assembled multilayered structures are popular functional coatings [1]. These are obtained by the successive construction of layers of materials on top of each other, *i.e.* through Layer-by-Layer (LbL) assembly. In the modern scientific community, the LbL nomenclature exists since the late 1960's and usually stands for the alternate adsorption of oppositely charged materials. The driving force of the multilayer growth is the surface charge overcompensation by the new layer of material that is adsorbed. This results in a surface charge inversion, which allows adsorbing a next layer of oppositely charged material. Charged soluble polymers, *i.e.* polyelectrolytes (PEs), are the most widely used materials. Their LbL assembly was first formalized and demonstrated by Decher et al. in 1992 by alternately dipping a supporting material into a solution of positively- and negatively-charged PE (see Fig. 1) [2]. The assembly is achieved according to the following sequence of steps: first, a supporting material is immersed in a solution of a positively-charged PE, *i.e.* a polycation, which adsorbs readily. Then, a washing step enables to remove loosely attached PE. Then a negatively charged PE, *i.e.* a polyanion, is adsorbed on the now positively-charged surface and subsequently washed as well (see Fig. 1). Note that the sequence can also start with the polyanion. By repeating this procedure, a PE multilayer (PEM), whose thickness can be precisely controlled by the number of adsorption cycles, is obtained [3]. This self-assembled layered structure can be obtained only by alternating the adsorption of PEs. The very same components adsorbed simultaneously would fail to self-assemble into a multilayer. A LbL assembly is thus an out-of-equilibrium self-assembly and the ability to create a multilayered architecture at interfaces has emerged from the pathway that was used to introduce the different components in the system. In terms of simplicity and versatility, the LbL assembly of PE holds the best promises for surface functionalization, especially compared to methods such as covalent binding. However, in terms of functionality, it is usually restricted to the chemical functions brought by the PEs and the multilayered structure (the latter gives particular light-material interactions for instance) that is obtained. Therefore, over the past thirty years, a myriad of other charged materials such as nanoparticles, lipids, nanosheets, DNA, proteins, *etc.* has been assembled using the LbL approach and the method has taken many different forms [1].

Proteins were amongst the first building blocks to be LbL-assembled. Only three years after the first paper published by Decher et al.

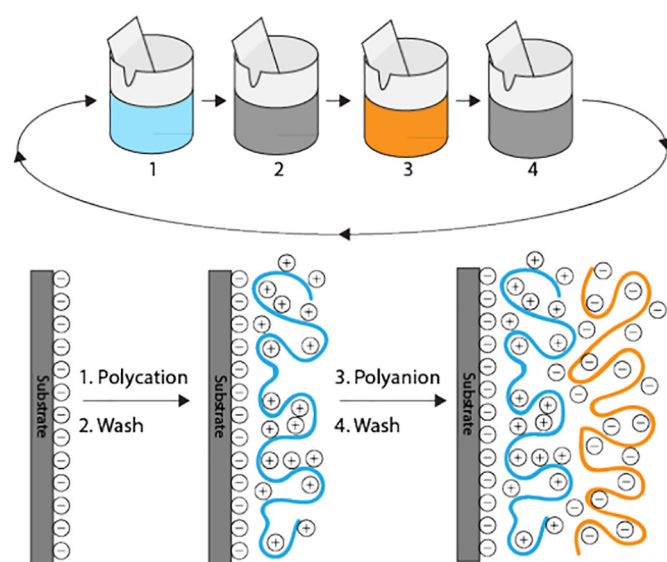


**Fig. 1.** Adapted from Decher et al. [4]: Schematic of the LbL film deposition process. Steps 1 and 3 represent the adsorption of a polycation and polyanion, respectively, and steps 2 and 4 are washing steps. Counterions are omitted for clarity. The polyanion conformation and layer interpenetration are an idealization of the surface charge reversal with each adsorption step.

on the LbL assembly of PEs, seven different globular proteins were immobilized by alternate adsorption with homo-PEs on surfaces [5,6]. Proteins are polymers of different amino acid residues. These residues can be either neutral, positive or negative depending on the pH. Proteins are thus a class of PEs since they are charged and usually soluble in water. For clarity, the word “protein” will be used in this review to designate polymers of different amino acid residues that folds into a 3D structure, therefore excluding homo-PEs made with amino acids such as poly-L-lysine or polyarginine, or small amorphous polypeptides. On the other hand, “PE” will refer to any soluble charged macromolecule that is not a protein. Poly-L-lysine and polyarginine will thus fall in the latter category.

With these first reports, the basic principles of the LbL assembly of PEs were applied to protein LbL assembly, *i.e.* alternate adsorption of oppositely charged building blocks and charge overcompensation. In order to fully grasp how the LbL assembly of proteins with PEs has evolved since its first use, and what are the challenges associated with this method, an extensive literature review is presented here. Entrapment of proteins in multilayered vesicles, diffusion of proteins in pre-formed solely PE-based multilayers and post-functionalization of LbLs with proteins were excluded. The LbL formation on nanostructured surfaces or on nano-objects were also excluded since these geometries highly influence the LbL construction. Then, all papers presenting sufficient data to conclude that a multilayer is growing were selected, *i.e.* papers in which the alternate adsorption of a protein with a PE was reported without further characterization of the obtained system were excluded. This finally represents 71 references that reported 119 different systems immobilizing 41 globular proteins/peptides and 5 proteins from the extracellular matrix. All these reported successful LbL assemblies are summarized in Table 1, with the respective pH and salt conditions used.

From this literature review, it appears that, within the ten years that followed the first protein immobilization by alternate adsorption with a PE, the LbL assembly of 17 supplementary globular proteins assembled with different PEs was reported. The vast majority of these proteins were enzymes. The main goal of these papers was to understand how proteins can be LbL-assembled with a PE and what is the effect of their immobilization on both their conformation and bioactivity. With that effort, systems that are useful for biosensing and heterogeneous biocatalysis were developed. In 2001, type-I collagen, a fibrillar protein from the extracellular matrix, was immobilized to promote interactions with cells. In the next five years, the LbL assembly of proteins of the extracellular matrix was developed to create new biomaterials [7]. However, up to now, only a few more proteins of the extracellular matrix were assembled with a PE, *i.e.* type-I and type-IV collagen, laminin, fibronectin and type-A gelatin (see Table 1). Importantly, many of the papers reporting the LbL assembly of extracellular matrix proteins with PEs lack a complete investigation of the multilayer growth, and the formation of a multilayer is assumed based solely on the alternate adsorption of oppositely charged species (which is purely speculative). These were not taken into account in this review. Interestingly, when analyzing with Scopus the number of documents published with “Layer-by-Layer AND (protein OR biomaterial)” in their title, abstract or keywords, it appears that a constant number of new documents is published since 2010. On the contrary, the number of new documents published with only “Layer-by-Layer” in their title, abstract or keywords has increased each year since 2010. This suggests that the field of LbL assembly for protein immobilization did not expand as well as the LbL field in general (see Fig. 2a). This observation is actually consistent with the decreasing number of new proteins that were successfully immobilized using the LbL approach between 1990 and 2017 (see Fig. 2b which is based on Table 1). It is reasonable to assume that the quality of the reports did not decrease with time. Therefore, the observed decreasing number of new proteins successfully immobilized comes from the limits of the conventional LbL method in immobilizing proteins rather than a decreasing number of papers presenting sufficient data to conclude that a multilayer is growing.

**Table 1**

Summary of all proteins successfully assembled using the LbL approach. Systems are reported as protein/PE and conditions are reported as *condition for protein assembly/condition for PE assembly* (if these conditions are different from each other). pH and salt used are separated by a coma. Only papers that demonstrate a LbL growth are reported. A list of abbreviations is provided below the Table.

Protein	System and conditions	Ref	Supporting material	Type of PEM growth
Globular				
Acylase (Acy)	<b>Acy/PEI</b> pH 8, tricine buffer	[59]	Planar	n.d.
Alcaline phosphatase (AIP)	<b>AIP/tannic acid</b> pH 5, 0.05 M acetate	[60]	Planar	n.d.
Alpha-amylase	<b><math>\alpha</math>-A/PEI</b> pH 6.9, 0.02 M PBS buffer with 6.7 mM NaCl	[59]	Planar	n.d.
Anti-platelet GP IIb/IIIa	<b>Anti-platelet GP IIb/IIIa/chitosan</b> pH 8 buffer, n.d./ pH n.d., 0.2 wt% acetic acid	[61]	Planar	Linear
Bacteriorhodopsin (BRh)	<b>BRh/poly-L-lysine</b> pH 7.2, DI water	[62]	Planar	n.d.
Beta-glucosidase (B-GLS)	<b>B-GLS/PSS</b> pH 4.8, 0.1 M Acetate buffer/ pH 4.8, 0.5 M NaCl	[63]	Spherical latex particles	n.d.
BSA	<b>BSA/PDADMAC</b> pH 7, PBS/ pH n.d., 0.5 M NaCl or pH 5.6, DI water/ pH n.d., 0.5 M NaCl	[64]	Planar	n.d.
	<b>BSA/PLL</b> pH n.d., 0.5 M NaCl	[65]	Spherical polystyrene particles	n.d.
Bone Morphogenetic Protein-2 (BMP-2)	<b>BMP-2/PAA</b> pH 4–5, 0.1 M sodium acetate	[66–68]	Scaffold	Linear
	<b>BMP-2/PAE</b> pH 5.1, 0.1 M acetate buffer/ pH 5.1, 0.025 M acetate buffer	[69]		
	<b>BMP-2/chondroitin sulfate</b> pH 5.1, 0.1 M acetate buffer/ DI water	[69]		
Catalase (CAT)	<b>CAT/PSS</b> pH 5, 1 M potassium acetate	[51]	Planar	Linear
	<b>CAT/star-PDMAEMA</b> pH 7, n.d./ pH 6, 0.1 M NaCl	[50,70]	Planar	Linear, hybrid with GOx
Cholesterol oxidase (COX)	<b>COX/PEI</b> pH 6.3, 0.1 M phosphate buffer/ pH 6.3, 2 M KCl	[71]	Planar	Sigmoidal, saturation after 10 bilayers
	<b>COX/PDADMAC</b> pH 6.3, 0.1 M phosphate buffer/ n.d.	[72]	Planar	n.d.
	<b>COX/PAH</b> pH 7.5, 0.01 M Tris HCl buffer	[73]	Planar	Linear
Choline oxidase (ChO)	<b>ChO/ PDADMAC</b> pH 8, 0.1 M PBS/ n.d.	[74]	On carbon nanotubes	n.d.
	<b>ChO/PDADMAC</b> pH 8, 0.1 M phosphate buffer/ pH 7.4, Dulbecco's buffer	[75]	On electrode	Indirect evidence
	<b>ChO/PEI</b>			
Cytochrome C (Cyt C)	<b>Cyt C/PSS</b> pH 4.5, 4.8, pH adjusted with HCl	[5]	Planar	n.d.
Cytochrome P450 (Cyt P450)	<b>Cyt P450/PEI</b> pH n.d., 0.1 M PBS (4 °C)/ n.d.	[76]	Planar	Linear
$\kappa$ -casein (Ca)	<b><math>\kappa</math>Ca/PAA</b> pH 3, n.d.	[33]	Planar	Exponential then linear
	<b><math>\kappa</math>Ca/PSS</b> pH 3, n.d.		Planar	Linear
Basic fibroblast growth factor (bFGF)	<b>bFGF/alginate</b> pH 5, sodium acetate buffer	[77]	Planar	Exponential
	<b>bFGF/chondroitin sulfate</b> pH 7.4, PBS/ pH 5.6, 0.1 M NaCl	[78]	Planar	Linear
Glucoamylase (GA)	<b>GA/PEI</b> pH 5, DI water	[37]	Planar	n.d.
	<b>GA/PEI</b> pH 6.5, n.d.	[5]	Planar	n.d.
	<b>GA/PDADMAC</b> pH 6.8, n.d.		Planar	n.d.
Glucose dehydrogenase (GDH)	<b>GDH/PSS</b> <b>GDH/PASA</b> n.d.	[79]	Planar	Linear
Glucose oxidase (GOX)	<b>GOX/PAH</b> pH 6.8, 0.05 M HEPES buffer/ pH 4.8, 0.5 M NaCl	[80]	Spherical particles	n.d.
	<b>GOX/Star PDMAEMA</b> pH 6, n.d./ pH 6, 0.1 M NaCl	[81]	Planar	n.d.
	<b>GOX/PEI</b> pH 5, DI water	[37]	Planar	n.d.
	<b>GOX/PEI</b> pH 6.5, n.d.	[5,38]	Planar	Linear

(continued on next page)

Table 1 (continued)

Protein	System and conditions	Ref	Supporting material	Type of PEM growth
Glucose 6-phosphate dehydrogenase (G6PDH2)	<b>GOX/star-PDMAEMA</b> pH 6, n.d./ pH 6, 0.1 M NaCl	[50,70]	Planar Planar	Linear, hybrid with CAT n.d.
	<b>GOX/PDADMAC</b> pH 6.8, n.d.			
Glutathione reductase (GR)	<b>G6PDH2/PEI-Fc</b> pH 7.5, 0.1 M Tris-HCl buffer containing 3.3 mM MgCl <sub>2</sub> / DI water	[82]	Planar	Indirect evidence
	<b>GR/PEI-Fc</b> pH 7.5, 0.1 M Tris-HCl buffer containing 3.3 mM MgCl <sub>2</sub> / DI water	[82]	Planar	Indirect evidence
Hemoglobin (Hb)	<b>Hb/PSS</b> pH 4.5, pH adjusted with HCl	[5]	Planar	Linear
	<b>Hb/PEI</b> pH 9.2, n.d.		Planar	Linear
	<b>Hb/ dextran sulfate</b> DI water	[13]	Planar	Slightly exponential - drying between steps with N2
	<b>Hf3/PSS</b> pH 7, n.d.	[5]	Planar	n.d.
Horseradish peroxidase (HRP)	<b>HRP/PSS</b> pH 6.8, 0.05 M HEPES buffer/ pH 4.8, 0.5 M NaCl	[83]	Spherical particles	n.d.
	<b>HRP/QPVP</b> pH 7.5, 0.1 M PBS/ n.d.	[84]	Planar	n.d.
	<b>HRP/PSS</b> pH 5.5, acetate buffer/ pH n.d., 0.5 M NaCl	[85]	Planar	Linear QCM-D
	<b>HRP/ redox active PE</b> n.d.	[86]	On electrode	Indirect evidence
	<b>IgG/PSS</b> pH 7.5, I = 0.1 M (0.05 M HEPES + NaCl) or pH 6, I = 0.1 M (0.05 M MES + NaCl)/ pH 6, 0.01 M MnCl <sub>2</sub>	[25]	Planar	Linear
IgG	<b>IgG/dextran sulfate</b> pH 4, 0.05 M citrate	[20]	Planar	n.d.
	<b>IgG/PSS</b> pH 6, 0.05 M MES/ pH n.d., 0.5 M NaCl	[64]	Planar	n.d.
	<b>IgG/PMAA</b> pH 4.5, pH 5, pH 5.5, pH 6, 0.01 M phosphate buffer	[17]	Planar	n.d.
	<b>IgG/PAA</b> pH 4, pH 4.5, 0.01 M phosphate buffer		Planar	n.d.
	<b>Anti-HRP/dextran sulfate</b> pH 4, 0.03 M citrate	[87]	Planar	Linear
Keratin (K)	<b>K/PDADMAC</b> K/PAA DI water	[26,88]	Planar	n.d.
Lactate oxidase (LAX)	<b>LAX/PVP-Os-AA</b> pH n.d., PBS/ n.d.	[89]	Planar	Linear
Laccase (Lac)	<b>Lac/PAH-Os</b> pH 4.7, 0.1 M acetate buffer/ pH 8, n.d.	[90]	Planar	Only two layers
	<b>Lac/PDADMAC</b> pH 4.5, 0.05 M sodium acetate	[91]	Planar	Linear
Lignin peroxidase (LiP)	<b>LiP/PDADMAC</b> <b>LiP/PEI</b> <b>LiP/PAH</b> pH 6, 0.024 or 0.040 M acetate buffer	[92]	Planar	Slightly linear, strong desorption observed
Lysozyme (Lyz)	<b>Lyz/PSS</b> pH 3 (citrate buffer), pH 5 (acetate buffer), pH 7.5 (HEPES buffer), pH 9.6 (carbonate buffer), I = 0, 0.01, 0.2 or 0.8 M	[10]	Planar	Linear
	<b>Lyz/PSS</b> pH 4, pH adjusted with HCl	[5]	Planar	Linear
	<b>Lyz/PSS</b> pH 6, n.d.	[93]	Planar	Linear
	<b>Lyz/PMAA</b> pH 5, pH 5.5, pH 6, pH 6.5, from 0 to 4 M NaCl	[6,17]	Planar	Linear up to 10 layers
	<b>Lyz/PAA</b> pH 4, pH 4.5, pH 5, pH 5.5 pH 6, from 0 to 2.4 M NaCl			
Manganese peroxidase (MnP)	<b>MnP/PDADMAC</b> <b>MnP/PEI</b> <b>MnP/PAH</b> pH 6, 0.024 or 0.040 M acetate buffer	[92]	Planar	Slightly linear, huge desorption observed
Myoglobin (Mb)	<b>Mb/PSS</b> pH 4, 0.001 M NaCl	[6]	Planar	Linear growth
	<b>Mb/ dextran sulfate</b> DI water	[13]	Planar	Slightly exponential - drying between steps with N2
Organophosphorous hydrolase (OPH)	<b>OPH/PTAA</b> pH 7.3 (0.1 M KH <sub>2</sub> PO <sub>4</sub> and 0.1 M NaOH)/ pH 8.8 (0.1 M Tris and 0.1 M HCl)	[94,95]	Planar	n.d.
Ovalbumin (Ova)	<b>OVA/PLL</b> <b>OVA/PAE</b> pH 6, 0.1 M acetate buffer	[96]	Planar	Linear

Table 1 (continued)

Protein	System and conditions	Ref	Supporting material	Type of PEM growth
Polyphenol oxidase (PPO)	<b>PPO/PAH</b> <i>pH 6.6, 0.01 M Tris buffer</i>	[97]	Planar	Linear
	<b>PPO/Chitosan</b> <i>pH n.d., PBS</i>	[98]	Planar	Exponential
	<b>PPO/PDADMAC</b> <i>pH 7, PBS buffer</i>	[99]	n.d.	n.d.
Ribonuclease A (bovine pancreas) (RNase)	<b>RNase/PMAA</b> <i>pH 4.5, pH 5, pH 5.5, pH 6, 0.01 M phosphate buffer</i>	[17]	Planar	n.d.
	<b>RNase/PAA</b> <i>pH 4, pH 4.5, pH 5, 0.01 M phosphate buffer</i>		Planar	n.d.
Trypsin (Trp)	<b>Trp/PSS</b> <i>pH 7.4, 0.05 M Tris or 0.02 M CaCl<sub>2</sub></i>	[100]	Planar	n.d.
	<b>Trp/alginate</b> <i>pH 7.4, 0.05 M Tris or 0.02 M CaCl<sub>2</sub></i>		Planar	n.d.
Uricase (UOx)	<b>UOx/PAH</b> <i>pH n.d., 0.1 M borate buffer/ pH n.d., Dulbecco's phosphate-buffered</i>	[101]	Planar	Linear
Urease (U)	<b>U/PDADMAC</b> <i>pH 7.2, 0.02 M Tris-HCl buffer</i>	[91]	Planar	Linear
Vascular Endothelial Growth Factor (VEGF)	<b>VEGF/PAA</b> <i>pH 5.0, 1 M sodium</i>	[66]	Scaffold	Linear
	<b>VEGF/heparin</b> <i>pH 7.4, PBS/ pH 4.2, DI</i>	[102]	Planar	Indirect evidence of growth
Peptide Insulin	<b>Insulin/Star PDMAEMA</b> <i>pH 6, n.d./ pH 6, 0.1 M NaCl</i>	[81]	n.d.	n.d.
	<b>Insulin/Star PDMAEMA</b> <i>pH 7, n.d./ pH 6, 0.1 M NaCl</i>	[50,70]	Planar	Linear, hybrid with GOX/star-PDMAEMA, Cat/star-PDMAEMA
Fibrous Collagen type-1 (Col1)	<b>Col1/PSS</b> <i>pH 4.2, pH adjusted with HCl/ pH 4, pH adjusted with HCl</i>	[103,104]	Planar Planar	Sigmoidal, saturation at 10 bilayers Linear
	<b>Col1/HA</b> <i>pH 4.7, 0.1 M acetate buffer</i>		Planar	Sawtooth, thinner layers with d-Col1 compared to Col1
	<b>d-Col1/PSS</b> <i>pH 4.7, 0.1 M acetate buffer</i>		Planar	Linear up to 5 bilayers
	<b>Col1/HA</b> <i>pH 4, acetic acid/ pH 4, DI water adjusted with HCl</i>	[8]	Planar	Linear up to 9 bilayers
	<b>Col1/HA</b> <i>pH 4, 0.012 M HCl + 0.1 M acetate buffer/ pH 4, 0.082 M acetic acid</i>	[105]	Planar	Linear up to 9 bilayers
	<b>Col1/HA</b> <i>pH 4.7, n.d. acetate buffer</i>	[106]	Planar	Exponential
	<b>Col1/He (heparin)</b> <i>pH 4, 0.2 M acetic acid buffer/ pH 7, DI water</i>	[107]	Planar	n.d.
	<b>Col1/chondroitin sulfate</b> <i>pH 3, 0.2 M NaCl/ pH n.d., 0.5 M NaCl</i>	[108]	n.d.	n.d.
	<b>Col1/chondroitin sulfate</b> <i>pH 3, 0.15 M NaCl, 1 mM HCl/ pH 6, 0.15 M NaCl</i>	[31]	Planar	Saturate after 6 bilayers
	<b>Col1/heparin</b> <i>pH 3, 0.15 M NaCl, 1 mM HCl/ pH 6, 0.15 M NaCl</i>		Planar	Linear
	<b>Col1/heparin</b> <i>pH 4, acetic buffer solution, 0.14 M NaCl</i>	[109]	Planar	Exponential - drying between steps with N <sub>2</sub>
	<b>Col1/heparin</b> <i>pH n.d. 0.2 M acetic acid/ pH 7, DI water</i>	[110]	Planar	Linear
	<b>Col1/PDADMAC</b> <i>pH n.d., 0.1 M acetic acid/ pH 10, DI water</i>	[111]	Planar	Linear
Collagen type-4 (Col4)	<b>Col4/PAA</b> <i>pH 4, adjusted with HCl</i>	[39]	Nano-particles	Linear up to 10 bilayers
Fibronectin (Fn)	<b>Fn/Poly-D-lysine</b> <i>pH 7.4, 0.1 M PBS</i>	[36]	Planar	Linear up to 8 bilayers
Gelatin type-A (Ge)	<b>Ge/PEI</b> <i>n.d./ pH 7.4, n.d.</i>	[112]	Planar	Linear up to 8 bilayers
	<b>Ge/chitosan</b> <i>n.d./ pH 4, 0.1 M acetic acid and 0.14 M NaCl</i>		Planar	Linear up to 8 bilayers
Laminin-1 (Lm1)	<b>Lm1/chitosan</b> <i>pH 7.4, PBS/ pH 4, 0.1 M acetic acid and 0.14 M NaCl</i>	[112]	Planar	Linear up to 8 bilayers
	<b>Lm1/Poly-D-lysine</b> <i>pH 7.4, 0.1 M PBS</i>	[36]	Planar	Linear up to 8 bilayers

List of abbreviations used in the table: DI: deionized. n.d.: not defined. PAA: poly(acrylic acid), PAE: poly( $\beta$ -amino ester), PAH: poly(allylamine hydrochloride), PASA: poly(anilinesulfonic acid), PDADMAC: poly(diallyldimethylammonium chloride), PDMAEMA: poly(dimethylaminoethyl methacrylate), PEI: poly(ethylenimine), PEI-Fc: poly(ethylenimine)-ferrocene carboxylic acid, PLL: poly(L-lysine), PMAA: poly(methacrylic acid), PSS: poly(styrene sulfonate), PTAA: poly(thiophene-3-acetic acid), PVP: polyvinylpyrrolidone, PVP-Os-AA: polyvinylpyridine-Os(bispyridine)-co-allylamine, QPVP: quaternized poly(4-vinylpyridine).

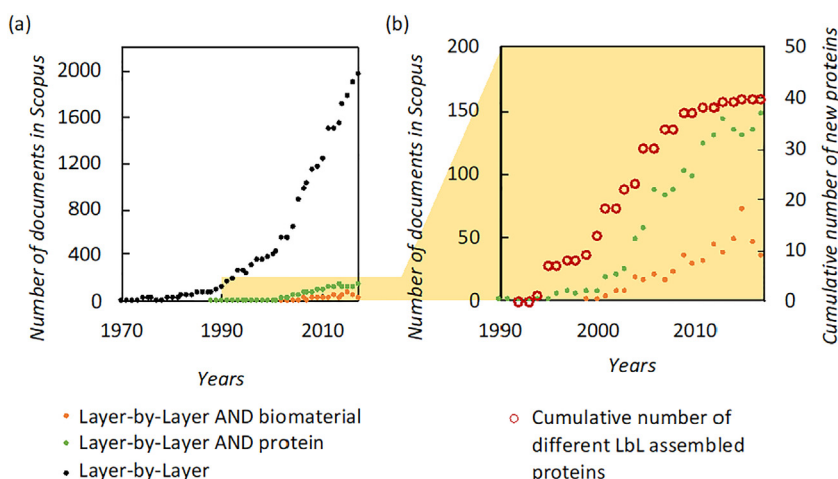


**Fig. 2.** (a) Evolution of the number of documents found in Scopus with the following word(s) in their title, abstract or keywords: Layer-by-Layer, Layer-by-Layer AND biomaterial, Layer-by-Layer AND protein. (b) Cumulative number of new proteins that have been reported to be LbL-assembled with a PE. Results presented together with a zoom corresponding to the yellow square of the left panel.

## 2. Strategies for the successful LbL assembly of protein with polyelectrolyte

The gap between the potential and the current state of the art of LbL assembly of proteins with PEs is clear and until now, there is no evident general way to immobilize any given protein by the LbL method. The difficulty is that the failure to grow a multilayer by alternating the adsorption of a protein with a PE is hardly reported, and usually only successful assemblies are presented. However, a few papers clearly show that the protein polyampholyte nature and complex 3D structure result in a lack of charge overcompensation upon multilayer growth. A telling example was presented by Zhang et al. for the LbL assembly of hyaluronic acid with type-I collagen. The surface charge was measured at each step of the multilayer construction and results are reproduced in Fig. 3a. It shows that, as the multilayer grows, the charge overcompensation, *i.e.* the number of unpaired charges, decreases [8]. To further highlight the role of protein heterogeneity on the growth of LbL assemblies, Mauquoy et al. assembled two proteins, namely type-I collagen and fibronectin. Three different buffers were tested as well as the influence of collagen denaturation and of a poly(ethylenimine) (PEI) anchoring layer. The total multilayer hydrated mass (expressed as a frequency shift) was measured as a function of the number of adsorption steps and results are reproduced in Fig. 3b. It appears that all studied conditions led to unsuccessful LbL assembly [9].

In order to illustrate the wide variety of protein structures, some of the proteins that are most used in LbL assemblies are shown at scale in Fig. 4. The charge distribution is critical for their LbL assembly. The protein surfaces were thus colored red for negative residues and blue for positive residues at physiological pH (the electrostatic surface potential of these proteins was calculated using the Chimera software and PDB structure). It appears that, for this rather small sample of proteins, a wide variety of size, shape and charge distribution is obtained. In all cases, the polyampholyte nature of proteins appears, with both positive and negative charges being present at their surface. To illustrate the charge distribution of type-I collagen while keeping the same scale as for other proteins, a collagen-like peptide is shown. Nevertheless, the low-resolution envelope structure of type-I collagen is presented in the bottom panel with all other proteins at the relevant lower resolution scale. The difference of size is striking, once more illustrating how diverse the protein structure can be. For the sake of comparison, a polystyrene sulfonate (PSS) chain is shown at scale for a polymerization degree of 340. The size of the random coil, *i.e.* the radius of gyration of PSS, was computed for the ionic strength ( $I$ ) of the human body fluid using

the same method as we presented elsewhere [10]. This also stresses the higher entropy and adaptability of the PE conformation compared to proteins. Another argument for the higher heterogeneity of proteins compared to PEs is that the former is made of the combination of 20 different a.a. amongst which only five are charged, while PEs are made from the repetition of only one (sometimes two) repeating unit bearing either a positive or a negative charge.

Due to this heterogeneity (charge nature, charge distribution, size, shape, chemical functions), proteins are extremely difficult to assemble LbL with a PE. In a view to facilitate the use of the LbL method for protein immobilization, a generic approach is presented in Fig. 5. The first step is to define the specifications of the application that is targeted. These specifications can be divided into two categories: the nature of the materials that are used and the functionalities that are desired. For the former, features of the PE and the protein (biodegradability, biocompatibility *etc.*) should be identified. For the latter, either multilayers that are stable (applications in biosensing or heterogeneous biocatalysis) or that release their content in a controlled manner (applications in drug delivery) are needed. These characteristics depend on the choice of the PE, but also on the building conditions (pH, salt concentration *etc.*). Once the specifications of the system are identified, the choice of the PE and the building conditions can be motivated *via* three distinct approaches that are represented in Fig. 5. These are based on the extensive literature review that was carried out (presented in Table 1).

1. Since protein structure (much more ordered when compared to PEs) and heterogeneity are thought to be the major limiting factors for their assembly, the first approach is to find a protein structural analog that was already successfully immobilized, and to use the same adsorption conditions and PE. In this view, the synthetic table of assembly conditions and protein/PE nature presented in Table 1 can be used. The reader willing to immobilize a new protein by the LbL method is thus invited to find structural analogs of that protein in this Table.
2. If no structural analog exists or if the analogous system does not self-assemble in a multilayer using the reported conditions, the prediction of the conditions that are necessary to grow a film based on the mechanisms of protein-PE LbL assembly may prove useful. All reported molecular driving forces of the LbL assembly have been reviewed extensively by Borges et al. [11] However, proteins were evidenced to exhibit a particular behavior when assembled with PEs using the LbL approach. This will be discussed hereafter.

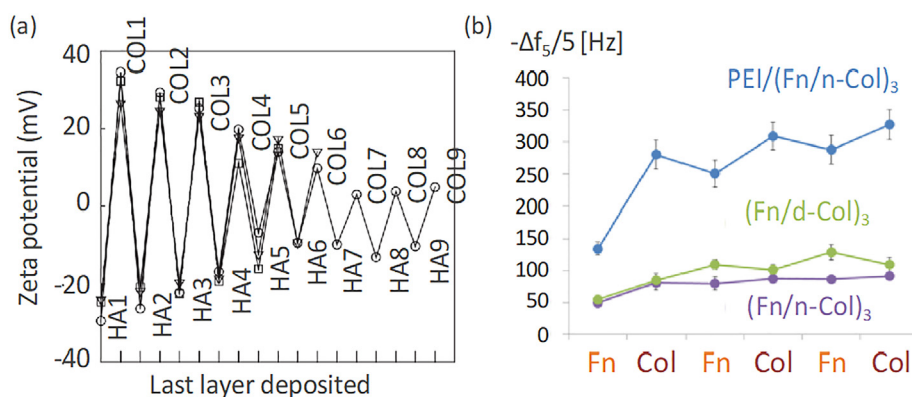


**Fig. 3.** (a) Evolution of the  $\zeta$  potential for three independent PEI/(HA/COL)<sub>n</sub> multilayer films during their construction. Reproduced from Zhang et al. with permission of Elsevier [8]. – (b) LbL assembly in phosphate buffer saline (PBS) of native type-I collagen (n-Col) with fibronectin (Fn) on a PEI anchoring layer (blue), denatured type-I collagen (d-Col) with Fn (green) or n-Col with Fn (purple). Reproduced from Mauquoy et al. with permission of Elsevier [9].

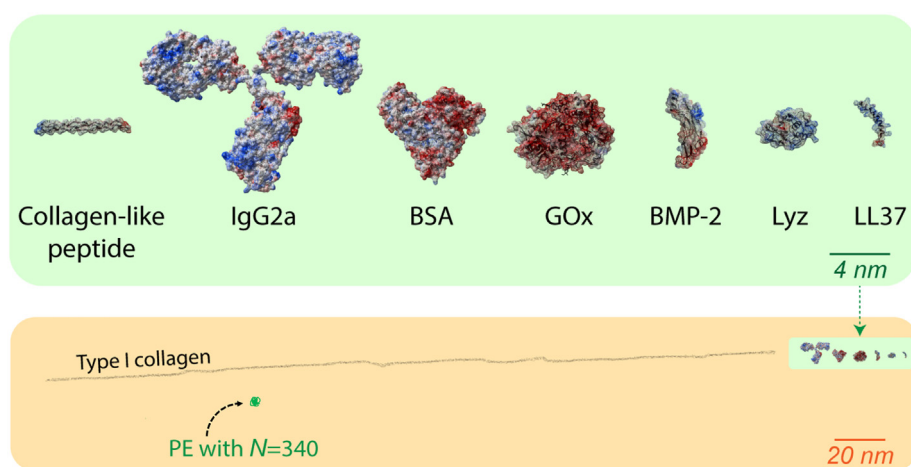


**Fig. 4.** Green box: molecular structure of type-I collagen (PDB: 3HQV), collagen-like peptide (PDB: 1CGD), IgG2A (PDB: 1IGT), BSA (PDB: 4F5S), GOx (PDB: 1GAL), BMP-2 (PDB: 3BMP), Lyz (PDB: 1HEL) and LL37 (PDB: 2K6O). The electrostatic surface potential is calculated using the Chimera software. The protein surface is colored red for negative potential and blue for positive potential. These molecular structures were produced using the UCSF Chimera package. – Orange box: type-I collagen is represented at scale with a PE (polymerization degree (N) of 340 – hypothetical fully extended chain conformation).

3. LbL assembly of protein crystals and of protein-PE complexes were both reported to allow the successful immobilization of proteins. These approaches permit to circumvent issues relative to the LbL assembly of proteins with PE and should be investigated as an alternative. Importantly, these LbL assemblies usually possess new features compared to classical LbL assemblies, which might be useful depending on the application. For clarity, such assemblies using protein-based particles will be referred to as unconventional LbL assemblies. They will be presented in the last section of this review.

### 3. Intrinsic and extrinsic parameters: Impact on the growth of protein-based multilayer films

In the following, the effect of two types of parameters on the protein-PE LbL assembly will be reviewed. The first type relates to extrinsic parameters, *i.e.* that are not specific to the desired multilayer (pH, nature and concentration of salts, temperature, concentration of protein and PE). The second type relates to intrinsic parameters, *i.e.* that defines the multilayer (nature and characteristics of PE, nature of the protein, effect of solid supporting material). The studies reviewed in this section were mainly conducted on planar surfaces (with a few exceptions regarding the  $\zeta$ -potential measurement of LbL-coated particles), for two main reasons. First, to avoid the effect of surface geometry. Second, to

allow the use of analytical methods such as quartz crystal microbalance with dissipation monitoring (QCM-D), atomic force microscopy (AFM), streaming potential measurements and X-ray photoelectron spectroscopy (XPS).

#### 3.1. Extrinsic parameters

##### 3.1.1. pH of the solution

pH was found to be a critical parameter in the very first paper reporting the LbL assembly of proteins with PE. It was shown that the pH of the protein solution has to be set apart from the isoelectric point (IEP) so that proteins are sufficiently charged in order to favorably interact with PE [5]. If the pH of the solution is adjusted lower than protein IEP, the protein will take a net positive charge. In this condition, the protein has to be LbL-assembled with a negative PE (see Fig. 6). If the pH of the solution is set above protein IEP, the opposite stands and the protein has to be LbL-assembled with a positive PE. This basic rule is represented in Fig. 6 for bovine serum albumin (BSA) that has a theoretical IEP of 5.78 and an experimental IEP of 4.7 [12]. The BSA charge was computed as a function of pH using its 3D structure (PDB structure of BSA: 4F5S) and the PDB2PQR server. It shows that the protein absolute charge increases when the pH of the protein solution deviates from the IEP (see Fig. 6). This is also represented by molecular graphics of

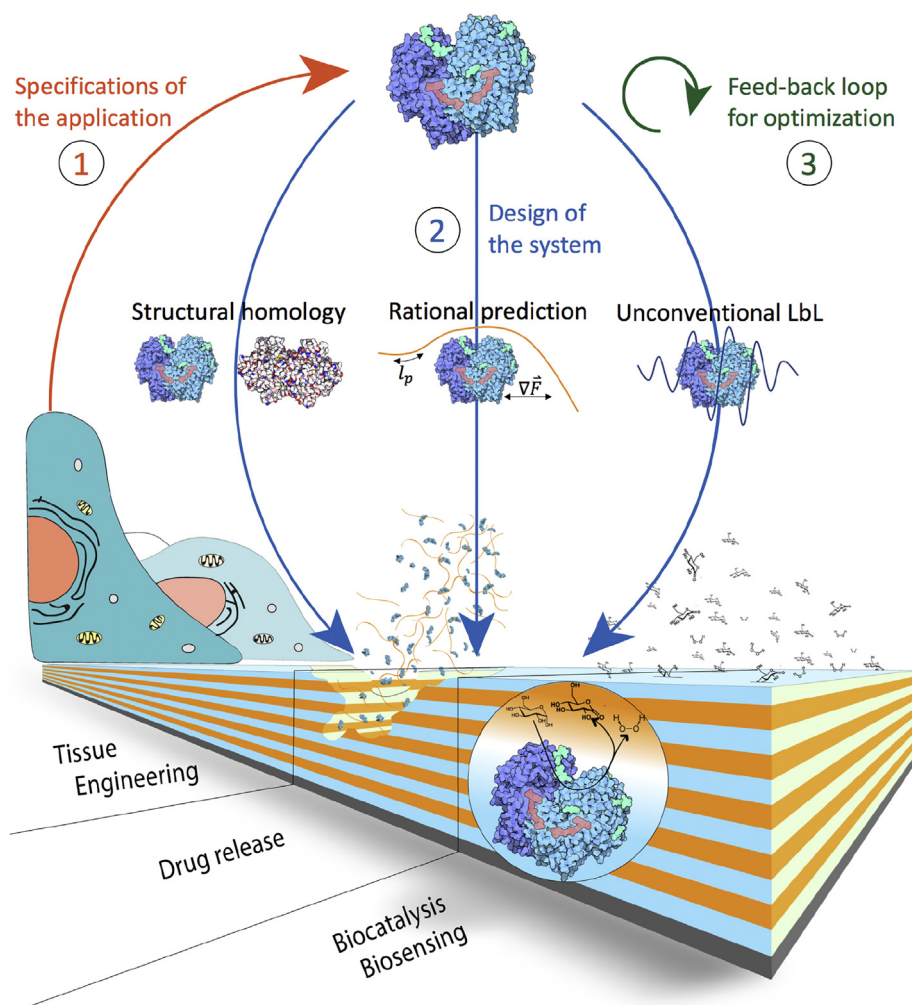


Fig. 5. Strategies to choose the right conditions and the right protein-PE couple for the LbL assembly of proteins. GOx and cyclooxygenase illustrations by David S. Goodsell and RCSB PDB.

BSA at different pH values in Fig. 6. The electrostatic surface potential of BSA was calculated using the Chimera software and colored red for negative potential, *i.e.* negative charge on the BSA backbone, or blue for positive potential, *i.e.* positive charge on the BSA backbone. BSA appears mainly positively charged in acidic pH and mainly negatively charged in alkaline pH. Importantly, around BSA IEP, the net charge is small while both positive and negative charges are present. Since the assembly relies on electrostatic interactions with a homogeneously charged PE, it is expected that working at a pH near the IEP of the protein would be detrimental for the LbL growth. The pH that is used for the LbL construction has thus to be chosen a few units above or below IEP. In order to support this affirmation, the difference between the protein IEP and the working pH value used for assembly,  $|pH - IEP|$ , was computed for different protein-based LbL films. Not all systems summarized in Table 1 provided sufficient data and only 72 systems were used. The results of this literature analysis are presented in Fig. 7. It appears that the vast majority (around 90%) of pH conditions that are used for the LbL construction with proteins are at least one pH unit above or below the protein IEP. This confirms that pH has to be fixed away from the protein IEP, and suggests that this condition should be maintained when designing a new system. This condition is represented as the broken black line in Fig. 7. Importantly, the protein was systematically alternately adsorbed with an oppositely charged PE. Only one paper reported the LbL assembly of a protein with a net charge of the same sign as the charges of the PE [13].

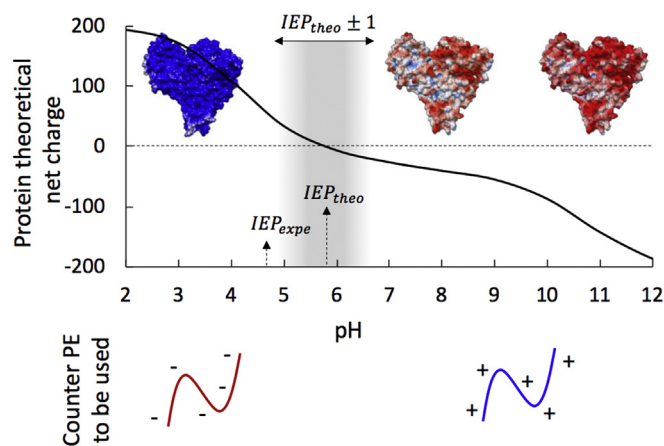


Fig. 6. BSA charge as a function of pH as computed from the PDB2PQR online tool and using the 4F5S PDB structure. The electrostatic surface potential of BSA is also calculated using the Chimera software. BSA is colored red for negative potential and blue for positive potential. The result is that, to perform LbL assembly, a counter polyanion has to be used below BSA IEP, and a counter polycation has to be used above BSA IEP. Note that BSA structure changes with pH and thus the molecular models presented here only illustrates the BSA surface charge variation with pH [14].

With respect to the protein charge variation with pH (as illustrated in Fig. 6), it has been reported that the higher the absolute net charge, the better the LbL assembly. Indeed, it was shown that more favorable electrostatic interactions improve LbL assembly [10,15]. In a similar way, it was shown that  $|pH - IEP|$  correlates with the protein amount that is adsorbed on an oppositely charged multilayer [16]. vander Straeten et al. demonstrated that the amount of lysozyme (Lyz) immobilized with a strong PE is proportional to Lyz charge [10]. The use of a strong polyacid discarded any PE conformation change with pH, which confirms the crucial role of the protein charge in LbL assembly. If a weak polyacid is chosen, the balance between protein and PE ionization governs LbL assembly. For example, it was shown that for Lyz assembled with poly(methacrylic acid) (PMAA), a weak polyacid, the immobilized amount highly depends on PMAA ionization degree [17]. Amongst others, it was shown that when PMAA has a high ionization degree, *i.e.* bears more negative charges, soluble Lyz/PMAA complexes form, thereby removing Lyz from the multilayer. This resulted in the failure to grow a LbL film.

The complexation in solution between proteins and PE that bears the same net charge has already been observed and attributed to the presence of positively-charged patches on the protein [18]. Interestingly, the LbL assembly of negatively-charged heme proteins with negatively-charged dextran sulfate was reported [13]. However, it might be that the N<sub>2</sub> drying step between each deposition step ensured LbL growth. Indeed, it appears in Table 1 that an exponential LbL growth (*i.e.* the mass increment increases at each step of the multilayer growth) is observed in most of the studies in which N<sub>2</sub> is used to dry the film between deposition steps. In contrast, when no drying step is used, the growth is usually linear (see Table 1). The complete change in the structure of the multilayer upon N<sub>2</sub> drying is supported by papers showing that when a PE layer is dried, further adsorption by a new immersion in the same solution is made possible (the same PE is thus adsorbed)

[19]. This latter case has been attributed to a rearrangement of the last adsorbed layer. It is thus clear that different LbL films are obtained when a drying step is applied between deposition steps. This might represent a valuable alternative if no LbL growth is achieved.

The pH value of LbL assembly has to be carefully selected so that protein denaturation does not occur. For example, hemoglobin assembled with PSS at pH 4.5 gets denatured while hemoglobin assembled at pH 9.2 with PEI retains its native structure [5]. Protein aggregation may also occur at given pH values as shown for the assembly of collagen with hyaluronic acid. In that case, the assembly has to be carried out at pH 4 to avoid fibril formation [8]. The pH of the multilayer construction should be selected with respect to the targeted application. Indeed, any change in condition may disrupt the formed film, especially when the PE or protein charge is decreased. In order to stabilize LbL films upon pH change, many papers reported on crosslinking strategies. Brynda et al. found that IgG could be assembled with dextran sulfate at pH 4 but an ELISA assay carried out at pH 7.4 disrupted the multilayer. The LbL film was thus crosslinked with glutaraldehyde after multilayer construction [20]. It is worth mentioning that while cross-linking improves multilayer stability, it may be detrimental to the protein functionality since it reacts with chemical functions present on its surface. Another potential cause for the loss of protein functionality/activity is the choice of the pH of LbL build-up. If  $|pH - IEP|$  is maximized to immobilize a large protein amount, it could lead to the construction of a multilayer which is too unstable to be used, except for drug delivery systems requiring a burst release. Indeed, the vast majority of proteins have an IEP which is close to the physiological pH (around pH 7, see Fig. 8). This suggests that lower or higher pH values should be chosen for LbL construction to maximize  $|pH - IEP|$ . However, the pH of the majority of applications is also found between pH 5 and pH 8. This is represented in Fig. 8 where the pH of different body parts is shown (data are taken from Lu et al. [21]), together with the IEP of proteins. This means

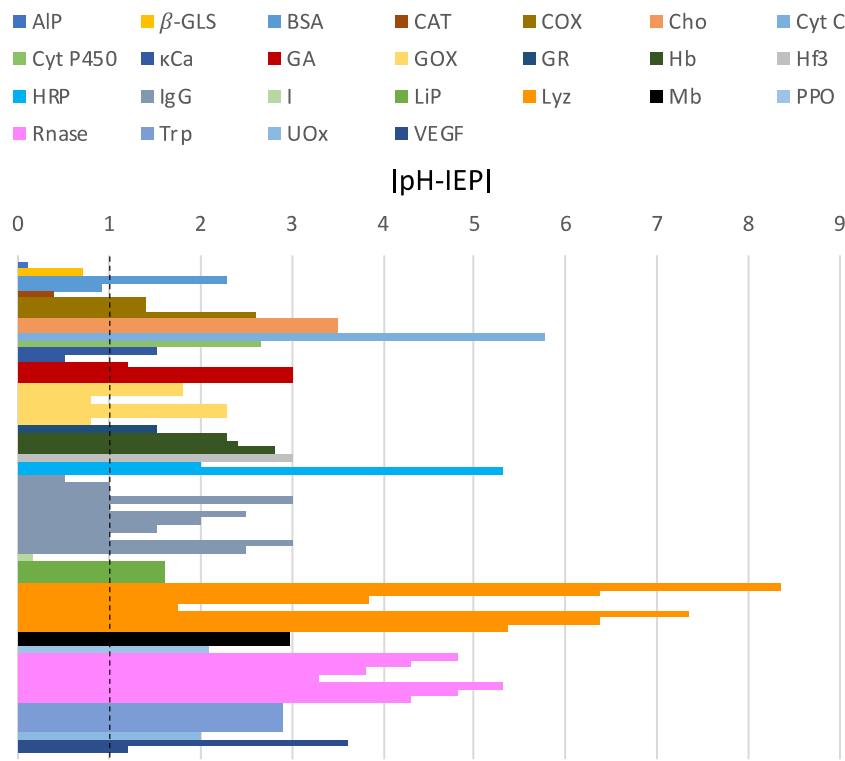


**Fig. 7.**  $|pH - IEP|$  was calculated for 25 different proteins successfully assembled in 72 different pH an I conditions using the LbL approach (using Table 1 when sufficient data were provided) – the pH value is the one selected for the protein adsorption step. Each colour represents a LbL-assembled protein (see Table 1 for the protein abbreviations). The protein IEP reported in the paper was used. If no IEP was reported, the theoretical IEP of the given protein was computed using PDB2PQR. In all cases reported in this Figure, the protein was oppositely charged to the PE.

that, after multilayer formation at a pH value far from the IEP, when the multilayer is placed in the conditions required for the application, the net charge of the protein decreases. The consequence is that the multilayer is likely to be disrupted. As an alternative, it could be interesting to construct the multilayer at the pH of the application. A lower protein amount would be immobilized, but a higher stability could be reached since the pH then does not change upon exposure to the medium. This comment is also valid for salt concentration, a parameter that will be discussed hereunder. With this in mind, alternative LbL assemblies such as those using protein-polyelectrolyte complexes as building blocks can be potentially useful since they were demonstrated independent of the protein charge, *i.e.* independent of the protein IEP [10]. These will be discussed in the last section of this review.

### 3.1.2. Presence of salts in solution

The presence of salts in solution has a tremendous influence on the multilayer growth. Similarly to pH, its effect on LbL construction of proteins with PE has been investigated since the first papers published on the subject. Ions dissolved in solution with proteins and PE have an influence on two length scales: on short distances through ion pairing, and on longer distances through Debye screening.

On short distances, it has been evidenced that ions are condensed on the charged functions of proteins and PE. These condensed counter-ions are released when the protein and the PE complex each other. Their

release produces an entropy gain, which favors the cooperative formation of ionic pairs between the protein and the PE. Curiously, this driving force is usually not discussed in the case of LbL assemblies with proteins. It is however considered as one of the major associative force driving the complexation of oppositely charged species [22]. It is also invoked in more details for soluble or suspended protein-polyelectrolyte complexes (PPCs) (*i.e.* not at interfaces).

On longer distances, the electrostatic screening of charges plays an important role in the LbL construction. [22–24] This screening can be evaluated by computing the Debye length ( $\kappa^{-1}$ ), which represents the distance over which electrostatic interactions are significant.  $\kappa^{-1}$  was computed as a function of salt concentration, which was expressed as the square root of the I (see Fig. 9, details on computation can be found in reference [10]). It appears that  $\kappa^{-1}$  is inversely proportional to the  $\sqrt{I}$ . The Bjerrum length ( $l_b$ ), which represents the distance at which electrostatic interaction between two charges is equal in magnitude to the thermal energy, is also represented as the dashed line on Fig. 9. When  $\kappa^{-1}$  reaches values below  $l_b$ , the electrostatic contribution to the LbL growth is thus considered negligible. For biological applications, it is worth mentioning that the ionic strength in physiological condition is of 155 mM, which gives a  $\kappa^{-1}$  of 0.77 nm. In the latter case and considering electrostatic interactions, it is thus highly probable that a multilayer would disassemble except if other attractive forces take the lead or if the multilayer has been crosslinked.

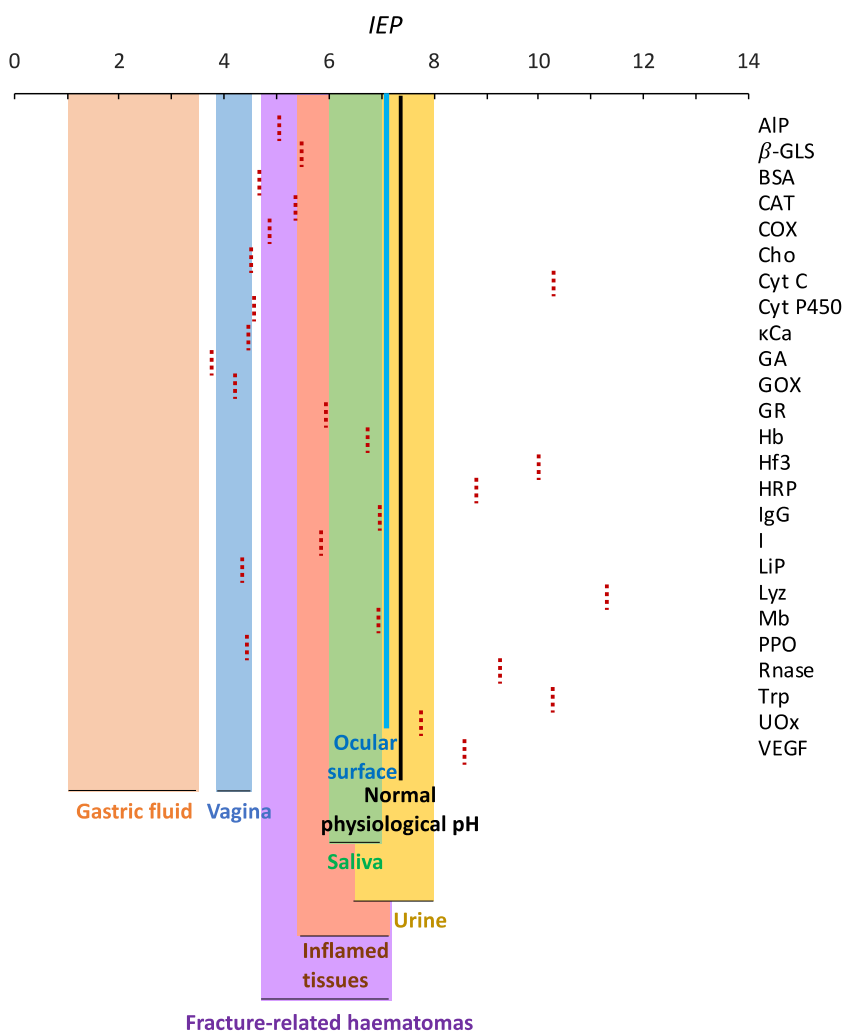
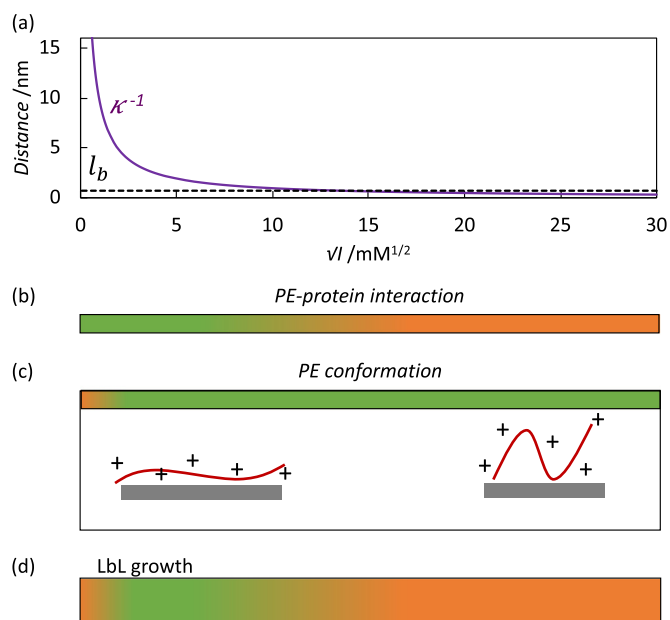


Fig. 8. IEP of proteins that were successfully LbL assembled represented as the dotted red line (data from Table 1). pH range of some body parts (pH data are taken from Lu et al. [21]).

Salt concentration also influences PE conformation, which is a key parameter in LbL construction. As represented in Fig. 9, when salt concentration increases, *i.e.*  $\kappa^{-1}$  decreases, the electrostatic repulsion between charged repeating units decreases and the PE becomes more flexible and adopts a more coiled structure in solution. The consequence is that polymer loops are formed upon adsorption on the surface for intermediate salt concentrations. In this way, Caruso et al. studied the effect of various  $\text{MnCl}_2$  amounts on the LbL deposition of poly(styrene sulfonate) (PSS) with anti-IgG on a poly(allylamine hydrochloride)-PSS ([PAH-PSS]<sub>2</sub>) precursor film [25]. They determined that increasing amounts of both PSS and anti-IgG were deposited with increasing  $\text{MnCl}_2$  concentration, *i.e.* 0, 10 and 100 mM  $\text{MnCl}_2$ . This observation was attributed to the more coiled PSS conformation as salt concentration rises. It was proposed that this coil conformation increases the surface available for anti-IgG adsorption, which was confirmed by the increased surface roughness with increased  $\text{MnCl}_2$  concentration [25].

The increased protein amount with increased salt concentration has also been attributed to the decreased lateral repulsion between adsorbed proteins. If the salt concentration decreases,  $\kappa^{-1}$  takes increasingly higher values and charged proteins repel each other. This results in a decreased protein density in each layer of a LbL film at low salt concentration [13].

Contrarily to what is observed when the salt concentration is increased from low to medium, the excessive charge screening at high  $I$  results in the impossibility to grow a film by alternate adsorption. For instance, type-1 collagen alternate adsorption with hyaluronic acid did not lead to any LbL growth at high salt concentration [8]. The same result was observed for keratin/poly(diallyldimethylammonium chloride) (PDADMAC) assembly that showed a decreased amount of immobilized keratin as salt concentration rose [26]. In a similar way, it has been shown that human serum albumin (HSA) adsorption on a multilayer ending with oppositely charged poly(vinyl sulfonate) (PVS) was drastically reduced when adsorption was carried out in 1 M NaCl instead of PBS buffer ( $I$  around 0.015 M) [16]. Additionally to charge screening, recent data suggest that the impossibility to grow a LbL film in concentrated salt solution is due to a decreased strength of the entropic contribution of ion pairing [27].



**Fig. 9.** (a)  $\kappa^{-1}$  (solid purple line) and the  $l_b$  are calculated as a function of salt concentration, which is expressed as the square root of  $I$ . (b) Favorable (green) and unfavorable (orange) electrostatic attraction between the protein and the PE depending at high and low  $I$ . (c) Schematics of the adsorbed PE conformation at low and high  $I$  and its expected contribution to the LbL growth. (d) Combination of PE-protein attraction and PE conformation contributions to the LbL growth.

In conclusion, the effect of salt on the LbL growth is non-monotonic (see Fig. 9). When salt concentration increases from low to medium, the PE becomes more flexible and lateral repulsion between proteins is screened. This results in an increased amount of protein incorporated in the LbL film as salt concentration rises. However, when salt concentration increases from medium to high, the electrostatic attraction decreases and the LbL growth is no longer possible. This was nicely shown by He et al. who studied the effect of a wide range of salt concentrations, and have shown that both the activity of the protein and the surface concentration of protein in LbL films increased then decreased with  $I$  (fixed with NaCl), passing through a maximum at about 300 mM NaCl [13]. More recently, it has been shown for the alternate adsorption of Lys with PSS, carried out at  $I = 0, 10, 200, 800$  mM, that maximal protein amounts were immobilized at  $I = 200$  mM [10].

Based on Table 1, all salt concentrations of the protein solutions that led to the successful LbL assembly of proteins with PE were collected and summarized as presented in Fig. 10a. In many studies, the reported condition was actually either not well defined or not even mentioned. This high proportion of missing information is stressed in Fig. 10a, where all missing data are presented as dashed blue squares. These raw data clearly suggest that the majority of the successful LbL assemblies were conducted at intermediate salt concentration. In order to clearly evidence this, the occurrence of each condition used in the range of less than 1, 1 to 49, 50 to 199 and more than 200 mM of salt was computed. Results are presented as histograms of the salt concentration in the protein solution and in the PE solution in Fig. 10b. It appears that LbL assemblies conducted at medium salt concentration are found twice more than others for successful LbL assembly. This analysis clearly supports that protein-PE LbL assembly proceeds better at intermediate salt concentration.

Multilayer stability as a function of salt concentration was also investigated. Indeed, it is common to construct multilayers in conditions that are different from the ones of their application. Usually, when  $I$  is increased above a certain value, the electrostatic screening of charges and salt doping disrupts the LbL film. Interestingly, the stability in salt solutions can be improved by forming hydrogen bonds in the multilayer. This can be done by changing the pH and protonating the PE. For example, a poly(acrylic acid) (PAA)-Lys multilayer was reported to be unstable when salt concentration was increased to physiological concentration at neutral pH while it was stable when  $I$  was increased at pH 5. This observation was attributed to the lower PAA ionization degree at lower pH resulting in the ability to form hydrogen bonds that stabilized the film [17]. As already mentioned, another way to improve multilayer is to crosslink the films.

### 3.1.3. Temperature

To our knowledge, the effect of temperature on the LbL assembly of proteins with PEs was not investigated. However, such assemblies share common features with LbL assemblies solely based on PEs (PEMs), and similar mechanisms are at play.

When a surface is immersed in a PE solution, the PE adsorbs on the surface through diffusion-driven kinetics. The rate of diffusion, which increases with temperature, thus dictates the time needed to reach equilibrium (the concentration also plays a role, which will be discussed later). When the temperature increases, the adsorption equilibrium is reached faster. This effect, which is observed in PEMs, is also expected in protein-PE LbL assemblies.

For some PEMs, PE adsorption for a given deposition step is not limited to the surface of the multilayer that is already formed and the PE can diffuse inside the multilayer. This PE diffusion in adjacent layers is also temperature dependent. Actually, the degree of PE interpenetration between layers is dictated by the ability of the PE to diffuse in the PEM, which depends on the PE-PE couple and on the conditions that are used [23]. If the PE interpenetration is constant at each step of the multilayer growth, the total multilayer mass increases linearly with the number of adsorption steps. Contrarily, if the deposited PE diffuses in the whole

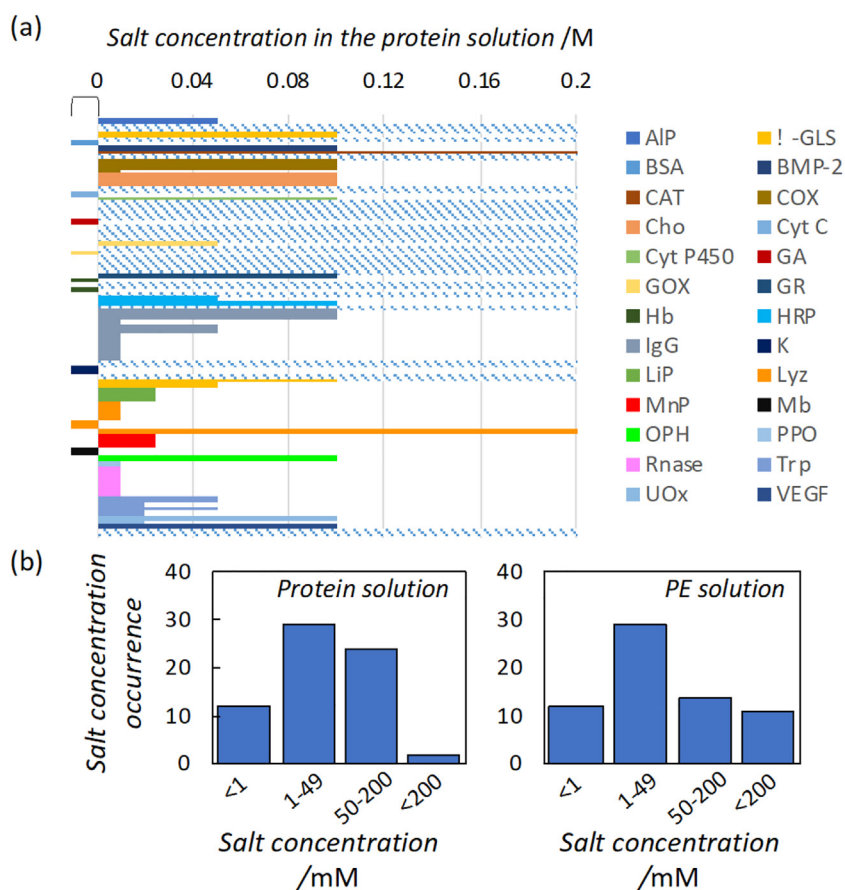


**Fig. 10.** (a) Overview of salt concentrations in the protein solution (alphabetical order) that were used to successfully immobilize various proteins. Lines on the left of the graph, under the header "0", are systems for which no salt was added. Dashed blue lines are data for which the pH was given (see Fig. 7), but the salt concentration was either missing or not sufficiently explicit. (see Table 1 for the protein abbreviations). (b) Histograms of the occurrence of the salt concentration used in the protein solution or PE solution. These histograms were constructed based on the values of (a), thus only based on studies in which salt concentration is explicitly reported. In the majority of the reports, the given materials and methods were not comprehensive enough to compute  $l$ .

multilayer, then the total multilayer mass increases exponentially with the number of adsorption steps. Using QCM-D, Vidyasagar et al. have shown that multilayers growing exponentially exhibited thermal transitions akin to a glass transition, while multilayers growing linearly were glassy and did not display such transition. They proposed that the glass transition is due to the great segmental mobility of PE [28]. Multilayers are thus highly dynamic and constantly reorganize upon adsorption of new charged materials [29]. The effect of temperature is that diffusion, *i.e.* interpenetration, in the PEM is improved, which results in a higher mass increment at each deposition step [30]. This may even lead to a transition between a linear and an exponential growth of the multilayer as temperature rises. With respect to protein-PE LbL assemblies, it is less likely that the protein may diffuse within the film given protein size. The PE used as the counterpolyion might, however, diffuse in the multilayer, which could improve LbL growth when temperature increases.

It is important to remind that protein fibrillation may occur at high temperature, which limits the temperature operation window. For instance, Mhanna et al. carried out collagen adsorption at 4 °C to avoid its fibrillation [31]. Another related issue is that temperature affects protein ternary structure and subsequently its activity.

### 3.1.4. Concentration of the protein solution

By analogy with PE-PE LbL assembly, one can assume that protein-PE growth is partially governed by protein diffusion. As for temperature, the increase of protein concentration in the solution that is used for the adsorption allows equilibrium to be reached faster. Besides kinetic, a

different protein concentration may allow to reach different equilibrium states. This parameter was only investigated in a few papers. It was reported that the amount of immobilized protein scales with protein concentration up to concentrations in the range of 1 mg mL<sup>-1</sup> [13]. He et al. tested the effect of different protein concentrations on their adsorption on a LbL film. The same adsorption time was used for all concentrations that were tested. A higher protein amount was observed on the multilayer surface when the concentration increased. This result was attributed to an incomplete surface saturation at low protein concentration, for the incubation time that was tested [13].

### 3.2. Intrinsic parameters

The rational prediction of LbL growth between proteins and PEs is very challenging due to the wide variety of parameters at play, and more importantly, due to the very high heterogeneity of proteins. Very few papers investigated systematically how the LbL film construction is affected by changing its composition, *i.e.* the PE nature (chemical nature, persistence length, charge) and the protein nature, as well as by changing the supporting material.

#### 3.2.1. Nature of the PE

When PEs are assembled LbL with proteins, they should be highly flexible to accommodate for the protein structure and form loops at the interface. The PE flexibility can be evaluated by its persistence length ( $l_p$ ), which represents the length over which correlation between PE segments is lost [32]. It was proposed that assembly is more

favorable when the  $l_p$  of PE is of the order of magnitude of the protein size [10].  $l_p$  is usually decomposed in the intrinsic persistence length ( $l_p^0$ ) and the electrostatic persistence length ( $l_p^e$ ).  $l_p^0$  represents the stiffening coming from steric hindrance and hybridization state of the atoms.  $l_p^e$  represents the stiffening due to electrostatic repulsion between charged repeating units. The latter parameter is thus related to  $\kappa^{-1}$ .

PEs with a small  $l_p^e$  must be selected to ensure PE flexibility. Then,  $l_p^0$  must also be kept with a small value. This can be achieved by increasing the salt concentration, i.e. by decreasing  $\kappa^{-1}$ . This will decrease the electrostatic repulsion between the repeating units and thereby increase PE flexibility. Polymers with a decreased number of charged repeating units can also be chosen. For instance, the degree of charged repeating units can be controlled in chitosan by its deacetylation degree. Finally, weak PEs can be chosen as pH allows to tune their ionization degree. When the PE is fully ionized, the repulsion between its repeating units will stiffen the PE chains.

The second feature of PEs that has to be considered is the nature of the charged group. At the molecular level, the association between oppositely charged PEs occurs through the cooperative formation of ionic pairs [23]. The free energy of this association, i.e. of complexation, is generally accepted to originate from an entropic contribution due to the loss of counter-ions and, to a lesser extent, from the enthalpic contribution coming from water perturbation [22]. Depending on the nature of the charged groups and of the counter-ions, the interaction between the polyanion and the polycation may thus vary. In this way, it has been shown in solution that PE-PE free energy of complexation scales with the Hoffmeister series. A PE side chain with a carboxylic acid function will thus interact more strongly with a polycation than a PE with a sulfonate function [22].

The ability of PEs to form hydrogen bonds with proteins is also critical for LbL formation. Lee et al. observed a linear growth for the LbL assembly of  $\kappa$ -casein with PSS. In contrast, when  $\kappa$ -casein is LbL-assembled with PAA, an exponential growth followed by a linear growth is observed [33]. Much thicker multilayers are thus obtained when PAA is used as shown in Fig. 11. This effect was attributed to the ability of PAA to form hydrogen bonds with  $\kappa$ -casein. The same effect was observed for Lyz LbL-assembled with PAA at various pH values [17].

Finally, the hydrophobicity of the PE plays an important role in the LbL construction. For instance, Cytochrome C was successfully LbL-assembled with PSS and poly(ester sulfonic acid) at a pH close to its IEP. The authors suggested that the hydrophobic interactions were involved in the build-up process since the protein net charge was close to zero [34]. Importantly, the authors stressed that the LbL construction is, however, not only based on one type of interaction but rather on an interplay of all of them [34]. The possible protein-PE interactions arise from van der Waals forces, hydrogen bonds, electrostatic forces and hydrophobic effects [35]. It is also worth to stress that protein interactions with hydrophobic PE could denature them. Indeed, PE interaction with apolar side chains of amino acid residues that are buried in the protein could alter protein structure and therefore its bioactivity.

### 3.2.2. Nature of the protein

The effect of the protein nature on LbL assembly is almost a case-by-case parameter due to the extremely large number of different structures of proteins. Even though some parameters such as geometrical features, tendency to unfold upon adsorption (soft versus hard protein) or charge distribution may guide the prediction of their LbL assembly, the absence of a systematic reporting of the failure to grow a LbL makes it hard to identify general rules. From the summary of all successfully immobilized proteins (see Table 1), it appears that the vast majority of these are globular. It is not straightforward to conclude whether this observation is due to a difficulty to immobilize fibrillar proteins or to a lower interest for the latter. As long as negative results are not systematically reported, the analysis of a large set of data from literature will be biased by the impossibility to differentiate correlation (a set of

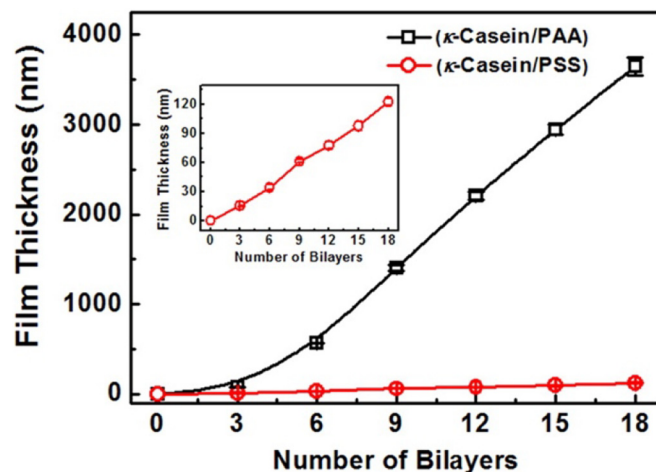


Fig. 11. Film growth behavior of ( $\kappa$ -casein/PAA) and ( $\kappa$ -casein/PSS) multilayered films assembled at pH 3 on silicon substrates by the dip-based LbL deposition. Inset: focus on ( $\kappa$ -casein/PSS) multilayers, showing the linear growth. Reprinted with permission from Lee et al. Copyright 2019 American Chemical Society [33].

protein is more interesting than another) from causality (a set of protein is easier to immobilize than another).

### 3.2.3. Supporting material

The chemistry of the supporting material is an important feature that highly dictates the LbL growth. However, this parameter is usually underestimated and the growth obtained for instance on a gold QCM-D sensor is extrapolated to other materials with different chemical surface properties without double checking that the same growth mechanism is still observed. The issue is that it is sometimes difficult, if not impossible, to obtain the same information with different methods since specific supporting material are required. The advantage that QCM-D offers is that the sensor can be coated with different materials. In this way, it was shown that collagen type-I/chondroitin sulfate growth on a QCM-D gold sensor is completely different from its growth on a poly(dimethyl siloxane) (PDMS)-coated sensor [31]. These results are shown in Fig. 12 and it appears that, on a gold sensor, collagen type-I adsorption is important for the first step and decreases in subsequent layers while, on a PDMS-coated sensor, the collagen type-I -chondroitin sulfate growth follows a linear path [31]. A less time-consuming approach that is used in most cases to circumvent a potential effect of the supporting material nature is the standardization of the surface through the construction of at least two PE-PE bilayers on the supporting material before further LbL construction [10,13,36].

## 4. Protein bioactivity in the LbL assembly

For most applications based on proteins, keeping their bioactivity intact after assembly is a key factor. The effect of their immobilization via LbL assembly will be reviewed hereafter.

The first proteins that were LbL-assembled with PEs are enzymes. It was rapidly evidenced that one of the main parameter limiting enzyme activity in LbLs is the substrate diffusion through the film [37]. For example, glucose oxidase (GOx) assembled with a PE on top of glucoamylase (GA), also assembled with a PE, showed different activities as a function of the nature of the last layer and the presence of a spacer between layers. In this case, a higher activity was observed when the enzymes were in the order of the cascade reaction, i.e. GA on the top that hydrolyses starch to glucose, which then reacts with GOx further in the multilayer. With respect to the influence of the spacer, it was shown that thicker spacers led to a higher activity, which may sound counterintuitive. It was proposed that, in this

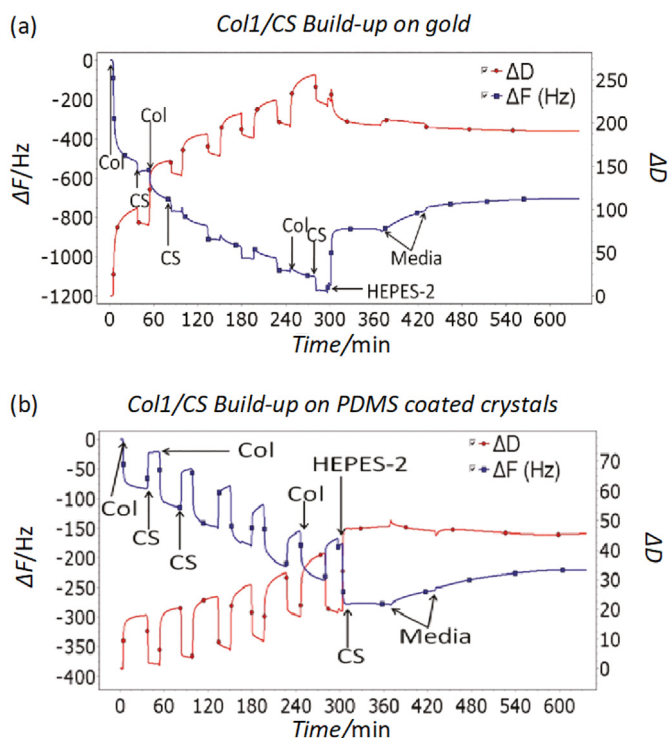


**Fig. 12.** Collagen type-I (Col1) - chondroitin sulfate (CS) build-up on (a) gold sensor or (b) PDMS coated sensor. Reprinted with permission from Mhanna et al. Copyright 2019 American Chemical Society [31].

particular case, a better enzyme-PE assembly is obtained on the spacer, or that  $\text{H}_2\text{O}_2$  produced by GOx, which inhibits both GA and GOx, diffuses more easily in a thin spacer [37]. It is however important to point out that this paper lacks experimental evidence on the stability of the enzyme in the layer. The measured enzymatic activity can be due to enzymes that are released from the film. The same group later reported the LbL assembly of GOx with PEI and PDADMAC. In this case, the activity was limited by substrate diffusion after the deposition of 2 layers of GOx-PEI. It was also shown that by changing the buffer, 40% of GOx can be released and that the enzyme that is released keeps about 80% of its native activity. Moreover, it was shown that GOx thermostability was improved through immobilization in LbL films [38]. Another example of how diffusion can influence activity in multilayers was reported with the diffusion of IgG in a LbL film formed with an anti-IgG and PSS [25]. It was shown that IgG is able to diffuse in the PSS-anti-IgG multilayer but fails to diffuse when each anti-IgG layer is separated by [PSS-[PAH-PSS]<sub>2</sub>] layers.

Another class of proteins that has been integrated in multilayers are proteins from the extracellular matrix (ECM). Such an approach is typically needed to build mimics of the ECM. Most of these studies reported the LbL assembly of collagen with a counter polyanion. It was consistently reported that collagen improves the biocompatibility by promoting cell adhesion and/or differentiation, and is able to limit the cytotoxicity of the supporting material. For example, it was reported that collagen type-I/PAA LbL assemblies promote cell attachment and survival on, otherwise, cytotoxic nanoparticles [39]. The order of the layers is important. Indeed, it was reported for collagen type-I/hyaluronic acid multilayers that chondrosarcoma cells produce their own extracellular matrix on collagen type-I-terminated films whereas such production is not found on hyaluronic acid-terminated ones.

Since the vast majority of proteins that were LbL assembled were enzymes, these types of multilayers have found applications in biosensing. Nevertheless, few studies reported the release of active proteins for biomedical application [40–43]. Especially, coated polymer microneedles are used for the transdermal delivery of protein, and implantable materials coated with growth factors improve both the osteointegration and the cell response [40,44–50].

### 5. Protein crystals and protein-PE complexes as building blocks for assembly

A way that was proposed to improve the LbL assembly of proteins with PEs is rather old. It was found in 2001 by Jin et al. that the LbL assembly of catalase with PSS results in poor film growth and poor enzymatic activity (see Fig. 13) [51]. As an alternative, microcrystals of catalase were created and coated with PSS. The resulting PSS-coated catalase crystals were then LbL-assembled with PAH. This methodology resulted in a much better film growth compared to the one based on uncoated catalase (soluble, i.e. not the crystalline form, see Fig. 13) [51]. It was also demonstrated that uncoated catalase crystals could not be assembled LbL with PAH without the prior formation of a PSS coating. It was proposed that the formation of a PSS coating allowed the LbL construction to rely on the PSS-PAH interaction rather than on the PSS-catalase interaction. This was proposed to be at the origin of the multilayer growth improvement. Especially, Jin et al. suggested that the higher negative charge density of PSS deposited on the enzyme crystals compared to the bare catalase molecules enabled a better LbL assembly. In other words, when the LbL assembly relies on PE-PE interaction rather than on protein-PE interaction, the multilayer growth is improved. A severe pitfall of this method is that protein crystals have to be obtained.

Actually, LbL build-up with components mixed with polyelectrolytes prior to assembly has been proposed in the early ages of the LbL method development [52–55]. This was proven to be effective for polyelectrolyte-polyelectrolyte complexes (PECs) [56]. Polyallylamine-poly(acrylic acid) (PAH-PAA) complexes, assembled in solution at different

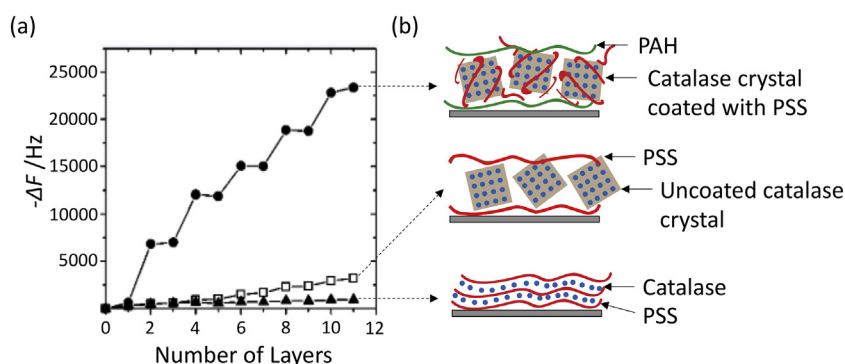


**Fig. 13.** (a) The frequency shift measured by QCM-D as a function of the number of layers for PSS-coated catalase crystals (circles), uncoated catalase crystal (square), solubilized catalase (triangles). These are alternately adsorbed with PAH or PSS. Reprinted with permission from Jin et al. Copyright 2019 American Chemical Society [51]. - (b) Schematic of each multilayer.

polymer ratios, were immobilized with poly(styrene sulfonate) (PSS) by the LbL method, giving new film morphologies.

Recently, we have proposed to complex proteins with PE so that their surface properties can be standardized. In this way, the obtained protein-polyelectrolyte complexes (PPC) can be assembled through LbL assembly with another oppositely charged PE [10,57]. This procedure is represented in Fig. 14. It was shown, based on experimental and theoretical considerations, that when PPCs are used, the LbL construction mechanism only relies on PE-PE interactions. In contrast, the conventional bare protein molecule integration into LbL films highly depends on the protein charge state, which represents a major drawback given the protein-to-protein variety. When it is previously complexed with a PE, the protein can be integrated in the LbL film independently of its charge, therefore considerably simplifying the protein integration in LbL assemblies [10]. Moreover, the obtained films were proven to be much more hydrated, resulting in an improved enzymatic activity of the immobilized enzyme compared to conventional LbL films [57]. Besides, it was recently shown that these multilayers can self-reorganize when the pH takes a certain value, and that a high fraction of non-complexed protein is released from the multilayer. The result is that, when compared to a classical PE-protein self-assembly, the protein released from a PPCs-PE self-assembly maintains a significantly higher bioactivity [58]. These results stress the need for new types of LbL assemblies that features new properties.

## 6. Conclusions and future prospects

In this review, we proposed three different strategies, *i.e.* structural homology, rational prediction and unconventional LbL, to guide the choice of conditions to be used in order to assemble proteins with PE in a LbL fashion. For each of these strategies, we summarized the key features that allow successful LbL growth. With respect to the structural homology, a summary of proteins successfully LbL assembled with PE, and the conditions of the assembly were presented. In a view to predict the conditions to be used for a new protein-PE couple (no homologous system or failure with similar conditions), the mechanisms of LbL assembly that are particular to proteins were reviewed. Finally, unconventional LbL strategies circumventing issues related to proteins LbL assembly were presented. Importantly, these might also bring new functionality to the system. Besides the strategy used to guide the choice of conditions, it was stressed that the conditions of assembly also dictate important features such as the stability of the system. Indeed, depending on the application that is aimed, either a stable or unstable system

has to be obtained. Considering the specifications of the foreseen application, the three distinct strategies that were identified and discussed in this review can be used independently for any protein and any application. Protein immobilization in multilayer has already been proven topical for a variety of fields including biosensing, biocatalysis, biomaterials and drug delivery. However, the great potential of LbL protein assembly is currently limited by the available strategies. Indeed, the two first strategies proposed in this review aim at identifying more easily the conditions for optimum multilayer growth. They do not offer many options when the best condition cannot be used for a given protein (*eg* best pH or ionic strength values for assembly outside of acceptable range for that given protein) or when the multilayer stability does not meet the requirements of the foreseen application. There is thus an important need for new unconventional LbL assembly methods that allow the available conditions for successful multilayer growth to be extended, or new features (stability, responsiveness, *etc.*) to be obtained. Importantly, these new methods should provide ways to standardize protein properties in order to easily transfer them to other proteins.

Constructing LbL thin films is the simplest and most intuitive way to order molecules at interfaces – it is not surprising that it has been intensively used. However, this method suffers from this naive picture and multilayers are always represented with simple cartoons corresponding to the method rather than to the real structure of the self-assembly. This is fine, except when one then assumes that the multilayer is made of the constituents that were used to grow it, and that it possesses the structure depicted by the simplified cartoons. This review evidenced that the LbL assembly of proteins with PE is not straightforward at all and that alternating the adsorption of oppositely charged components is not sufficient to allow the growing of a film in a multilayered fashion. Moreover, when a multilayer is constructed, its composition and structure should always be fully investigated and cannot be predicted based on the method nor the constituents. Understanding the interactions and the competition between soluble and surface-immobilized compounds is of utmost importance, as well as taking care of effects related to subtle details of the assembly process.

Another consequence of this naive picture is that an incremental strategy is usually chosen when a LbL with specific functions is desired. With this strategy, a model LbL assembly is gradually improved to finally obtain the desired functions. This allows the use of materials that are not expensive or easy to detect to optimize the conditions that lead to a good LbL growth, a stable multilayer, or a multilayer that releases its content in a controlled manner. Then, the PE or the protein is replaced by the more expensive/less easy to detect constituent, or is

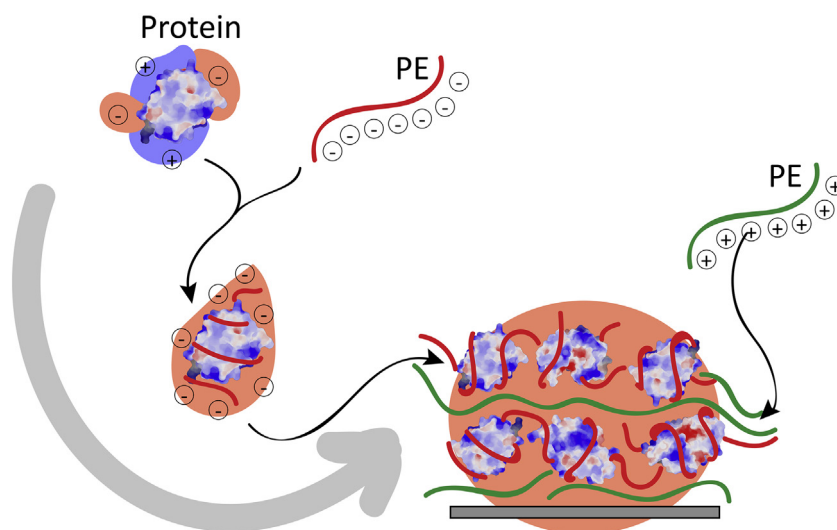


Fig. 14. Schematic representation of the complexation of a protein with a PE, and subsequent LbL assembly with an oppositely charged PE.

constructed on a different surface geometry that is required for the application. Note that the latter step usually stays at the proposal stage. As a matter of fact, the LbL systems that were presented in this review were mostly composed of proteins with limited biotechnological interest (there is a strikingly lower number of therapeutic proteins than “common” enzymes). This incremental strategy emerges from the laconic assumption that alternating the adsorption of oppositely charged species is the main driving force of the LbL self-assembly, and that any similar macromolecule would self-assemble the same way. However, the LbL assembly of proteins with PE depends on a wide range of parameters such as protein and PE nature and concentration, ions and counterions nature, adsorption sequence, temperature, solvent, surface geometry and chemistry, and each of which can drastically change the resulting multilayers. Thus, translation from the model to the application cannot be predicted. Therefore, materials (PE, protein, surface, etc.) that fully match the specifications of the targeted application must be chosen and used from the beginning, even if it sometimes makes the analysis of the composition, the stability and the structure more challenging. This approach is in line with new design strategies of materials science in general [21].

### Author contributions

The manuscript was written through contributions of all authors.

### Declaration of Competing Interest

The authors declare that they have no known competing financial interests or personal relationships that could have appeared to influence the work reported in this paper.

### Acknowledgment

The work was supported by BELSPO, the Belgian Science Policy, through the Interuniversity Attraction Pole Program (P07/05), by the Belgian National Foundation for Scientific Research (FNRS) and the Research Foundation for Industry and Agriculture (FRIA).

### References

- Richardson JJ, Björnalm M, Caruso F. Technology-driven layer-by-layer assembly of nanofilms. *Science* 2015;348:348. <https://doi.org/10.1126/science.aaa2491>.
- Decher G, Hong JD, Schmitt J. Buildup of ultrathin multilayer films by a self-assembly process: III. Consecutively alternating adsorption of anionic and cationic polyelectrolytes on charged surfaces. *Thin Solid Films* 1992;210–211:831–5. [https://doi.org/10.1016/0040-6090\(92\)90417-A](https://doi.org/10.1016/0040-6090(92)90417-A).
- Hoogeveen NG, Cohen Stuart MA, Fleer GJ, Böhmer MR. Formation and stability of multilayers of polyelectrolytes. *Langmuir* 1996;12:3675–81. <https://doi.org/10.1021/la951574y>.
- Decher G. Fuzzy nanoassemblies: Toward layered polymeric multicomposites. *Science* 1997;277(5330):1232–7. <https://doi.org/10.1126/science.277.5330.1232>.
- Lvov Y, Ariga K, Kunitake T, Ichinose I. Assembly of Multicomponent Protein Films by Means of Electrostatic Layer-by-Layer Adsorption. *J Am Chem Soc* 1995;117:6117–23. <https://doi.org/10.1021/ja00127a026>.
- Lvov Y, Ariga K, Kunitake T. Layer-by-Layer Assembly of Alternate Protein/Polyion Ultrathin Films. *Chem Lett* 1994;23:2323–6. <https://doi.org/10.1246/cl.1994.2323>.
- Tang Z, Wang Y, Podsiadlo P, Kotov NA. Biomedical applications of layer-by-layer assembly: From biomimetics to tissue engineering. *Adv Mater* 2006;18:3203–24. <https://doi.org/10.1002/adma.200600113>.
- Zhang J, Senger B, Vautier D, Picart C, Schaaf P, Voegel JC, et al. Natural polyelectrolyte films based on layer-by-layer deposition of collagen and hyaluronic acid. *Biomaterials* 2005;26:3353–61. <https://doi.org/10.1016/j.biomaterials.2004.08.019>.
- Mauquoy S, Dupont-Gillain C. Combination of collagen and fibronectin to design biomimetic interfaces: Do these proteins form layer-by-layer assemblies? *Colloids Surf B: Biointerfaces* 2016;147:54–64. <https://doi.org/10.1016/j.colsurfb.2016.07.038>.
- vander Straeten A, Bratek-Skicka A, Jonas AM, Fustin CA, Dupont-Gillain C. Integrating proteins in layer-by-layer assemblies independently of their electrical charge. *ACS Nano* 2018;12:8372–81. <https://doi.org/10.1021/acsnano.8b03710>.
- Wan J, Han J, Wang Y, Ni L, Wang L, Li C. Switch on/off of cellulase activity based on synergetic polymer pair system. *Biochem Eng J* 2017;126:1–7. <https://doi.org/10.1016/j.bej.2017.06.018>.
- Peters T. All about albumin: biochemistry, genetics and medical applications. Academic Press; 1995.
- He P, Hu N. Interactions between heme proteins and dextran sulfate in layer-by-layer assembly films. *J Phys Chem B* 2004;108:13144–52. <https://doi.org/10.1021/jp049974u>.
- Jachimska B, Pajor A. Physico-chemical characterization of bovine serum albumin in solution and as deposited on surfaces. *Bioelectrochemistry* 2012;87:138–46. <https://doi.org/10.1016/j.bioelechem.2011.09.004>.
- Wang B, Wang YJ, Gao XF, Li YS. Utilization of parameters developed in layer-by-layer fabrication of protein-containing films for enzyme immobilization. *J Biomater Sci Polym Ed* 2015;26:1312–26. <https://doi.org/10.1080/09205063.2015.1089656>.
- Müller M, Rieser T, Dubin PL, Lunkwitz K. Selective interaction between proteins and the outermost surface of polyelectrolyte multilayers: Influence of the polyanion type, pH and salt. *Macromol Rapid Commun* 2001;22:390–5. [https://doi.org/10.1002/1521-3927\(20010301\)22:6<390::AID-MARC390>3.0.CO;2-B](https://doi.org/10.1002/1521-3927(20010301)22:6<390::AID-MARC390>3.0.CO;2-B).
- Izumrudov VA, Kharlampieva E, Sukhishvili SA. Multilayers of a globular protein and a weak polyacid: Role of polyacid ionization in growth and decomposition in salt solutions. *Biomacromolecules* 2005;6:1782–8. <https://doi.org/10.1021/bm050096v>.
- Kayitmazer AB, Seeman D, Minsky BB, Dubin PL, Xu Y. Protein-polyelectrolyte interactions. *Soft Matter* 2013;9:2553–83. <https://doi.org/10.1039/c2sm27002a>.
- Cochin D, Laschewsky A. Layer-by-layer self-assembly of hydrophobically modified polyelectrolytes. *Macromol Chem Phys* 1999;200:609–15. [https://doi.org/10.1002/\(SICI\)1521-3935\(19990301\)200:3<609::AID-MACP609>3.0.CO;2-X](https://doi.org/10.1002/(SICI)1521-3935(19990301)200:3<609::AID-MACP609>3.0.CO;2-X).
- Brynda E, Homola J, Houska M, Pfeifer P, Škvor J. Antibody networks for surface plasmon resonance immunosensors. *Sensors Actuators B Chem* 1999;54:132–136. [https://doi.org/10.1016/S0925-4005\(98\)00331-1](https://doi.org/10.1016/S0925-4005(98)00331-1).
- Lu Y, Aimetti AA, Langer R, Gu Z. Bioresponsive materials. *Nat Rev Mater* 2016;2:16075. <https://doi.org/10.1038/natrevmats.2016.75>.
- Fu J, Schlenoff JB. Driving Forces for Oppositely Charged Polyon Association in Aqueous Solutions: Enthalpic, Entropic, but Not Electrostatic. *J Am Chem Soc* 2016;138:980–90. <https://doi.org/10.1021/jacs.5b11878>.
- Lowack K, Helm CA. Molecular mechanisms controlling the self-assembly process of polyelectrolyte multilayers. *Macromolecules* 1998;31:823–33. <https://doi.org/10.1021/ma9614454>.
- Glinel K, Moussa A, Jonas AM, Laschewsky A. Influence of polyelectrolyte charge density on the formation of multilayers of strong polyelectrolytes at low ionic strength. *Langmuir* 2002;18:1408–12. <https://doi.org/10.1021/la0113670>.
- Caruso F, Niikura K, Furlong DN, Okahata Y. 2. Assembly of alternating polyelectrolyte and protein multilayer films for immunoassaying. *Langmuir* 1997;13:3427–33. <https://doi.org/10.1021/la9608223>.
- Yang X, Zhang H, Yuan X, Cui S. Wool keratin: A novel building block for layer-by-layer self-assembly. *J Colloid Interface Sci* 2009;336:756–60. <https://doi.org/10.1016/j.jcis.2009.04.050>.
- Lounis FM, Chamieh J, Leclercq L, Gonzalez P, Geneste A, Prelot B, et al. Interactions between Oppositely Charged Polyelectrolytes by Isothermal Titration Calorimetry: Effect of Ionic Strength and Charge Density. *J Phys Chem B* 2017;121:2684–3694. <https://doi.org/10.1021/acs.jpcc.6b11907>.
- Vidyasagar A, Sung C, Gamble R, Lutkenhaus JL. Thermal transitions in dry and hydrated layer-by-layer assemblies exhibiting linear and exponential growth. *ACS Nano* 2012;6:6174–6184. <https://doi.org/10.1021/nn301526b>.
- Porcel C, Lavallo P, Decher G, Senger B, Voegel JC, Schaaf P. Influence of the polyelectrolyte molecular weight on exponentially growing multilayer films in the linear regime. *Langmuir* 2007;23:1898–904. <https://doi.org/10.1021/la062728k>.
- Salomäki M, Vinokurov IA, Kankare J. Effect of temperature on the buildup of polyelectrolyte multilayers. *Langmuir* 2005;21:11232–40. <https://doi.org/10.1021/la051600k>.
- Mhanna RF, Vörös J, Zenobi-Wong M. Layer-by-layer films made from extracellular matrix macromolecules on silicone substrates. *Biomacromolecules* 2011;12:609–16. <https://doi.org/10.1021/bm1012772>.
- Dobrynin AV, Rubinstein M. Theory of polyelectrolytes in solutions and at surfaces. *Prog Polym Sci* 2005;30:1049–118. <https://doi.org/10.1016/j.progpolymsci.2005.07.006>.
- Lee JH, Hwang HJ, Bhak G, Jang Y, Paik SR, Char K. In situ fibril formation of  $\kappa$ -casein by external stimuli within multilayer thin films. *ACS Macro Lett* 2013;2:688–93. <https://doi.org/10.1021/mz400276f>.
- Lojou É, Bianco P. Buildup of polyelectrolyte-protein multilayer assemblies on gold electrodes. Role of the hydrophobic effect. *Langmuir* 2004;20:748–55. <https://doi.org/10.1021/la030286w>.
- Salloum DS, Schlenoff JB. Protein adsorption modalities of polyelectrolyte multilayers. *Biomacromolecules* 2004;5:1089–796. <https://doi.org/10.1021/bm034522t>.
- Ai H, Meng H, Ichinose I, Jones SA, Mills DK, Lvov YM, et al. Biocompatibility of layer-by-layer self-assembled nanofilm on silicone rubber for neurons. *J Neurosci Methods* 2003;128:1–8. [https://doi.org/10.1016/S0165-0270\(03\)00191-2](https://doi.org/10.1016/S0165-0270(03)00191-2).
- Onda M, Lvov Y, Ariga K, Kunitake T. Sequential reaction and product separation on molecular films of glucoamylase and glucose oxidase assembled on an ultrafilter. *J Ferment Bioeng* 1996;82:502–6. [https://doi.org/10.1016/S0922-338X\(97\)86992-9](https://doi.org/10.1016/S0922-338X(97)86992-9).
- Onda M, Ariga K, Kunitake T. Activity and stability of glucose oxidase in molecular films assembled alternately with polyions. *J Biosci Bioeng* 1999;87:69–75. [https://doi.org/10.1016/S1389-1723\(99\)80010-3](https://doi.org/10.1016/S1389-1723(99)80010-3).
- Sinani VA, Koktysh DS, Yun BG, Matts RL, Pappas TC, Motamedi M, et al. Collagen coating promotes biocompatibility of semiconductor nanoparticles in stratified LbL films. *Nano Lett* 2003;3:1177–82. <https://doi.org/10.1021/nl0255045>.
- Keeney M, Jiang XY, Yamane M, Lee M, Goodman S, Yang F. Nanocoating for biomolecule delivery using layer-by-layer self-assembly. *J Mater Chem B* 2015;3:8757–70. <https://doi.org/10.1039/c5tb00450k>.

- [41] Ai H, Jones SA, Lvov YM. Biomedical applications of electrostatic layer-by-layer nano-assembly of polymers, enzymes, and nanoparticles, 39; 2003. <https://doi.org/10.1385/CBB:39:1:23> Humana Press.
- [42] Iost RM, Crespihlo FN. Layer-by-layer self-assembly and electrochemistry: Applications in biosensing and bioelectronics. *Biosens Bioelectron* 2012;31:1–10. <https://doi.org/10.1016/j.bios.2011.10.040>.
- [43] Siqueira JR, Caseli L, Crespihlo FN, Zucolotto V, Oliveira ON. Immobilization of biomolecules on nanostructured films for biosensing. *Biosens Bioelectron* 2010;25:1254–63. <https://doi.org/10.1016/j.bios.2009.09.043>.
- [44] Lin X, Choi D, Hong J. Insulin particles as building blocks for controlled insulin release multilayer nano-films. *Mater Sci Eng C* 2015;54:239–44. <https://doi.org/10.1016/j.msec.2015.05.046>.
- [45] Saurer EM, Flessner RM, Sullivan SP, Prausnitz MR, Lynn DM. Layer-by-layer assembly of DNA- and protein-containing films on microneedles for drug delivery to the skin. *Biomacromolecules* 2010;11:3136–43. <https://doi.org/10.1021/bm1009443>.
- [46] Zeng Q, Gammon JM, Tostanoski LH, Chiu YC, Jeswell CM. In Vivo Expansion of Melanoma-Specific T Cells Using Microneedle Arrays Coated with Immune-Polyelectrolyte Multilayers. *ACS Biomater Sci Eng* 2017;3:195–205. <https://doi.org/10.1021/acsbomaterials.6b00414>.
- [47] Kim NW, Lee MS, Kim KR, Lee JE, Lee K, Park JS, et al. Polyplex-releasing microneedles for enhanced cutaneous delivery of DNA vaccine. *J Control Release* 2014;179:11–7. <https://doi.org/10.1016/j.jconrel.2014.01.016>.
- [48] Ye Y, Yu J, Wen D, Kahkoska AR, Gu Z. Polymeric microneedles for transdermal protein delivery. *Adv Drug Deliv Rev* 2018;127:106–18. <https://doi.org/10.1016/j.addr.2018.01.015>.
- [49] Macdonald ML, Rodriguez NM, Shah NJ, Hammond PT. Characterization of tunable FGF-2 releasing polyelectrolyte multilayers. *Biomacromolecules* 2010;11:2053–9. <https://doi.org/10.1021/bm100413w>.
- [50] Tachikawa T, Yonezawa T, Majima T. Super-resolution mapping of reactive sites on titania-based nanoparticles with water-soluble fluorogenic probes. *ACS Nano* 2013;7:263–75. <https://doi.org/10.1021/nn303964v>.
- [51] Jin W, Shi X, Caruso F. High activity enzyme microcrystal multilayer films [3]. *J Am Chem Soc* 2001;123:8121–2. <https://doi.org/10.1021/ja015807l>.
- [52] Ariga K, Onda M, Lvov Y, Kunitake T. Alternate layer-by-layer assembly of organic dyes and proteins is facilitated by pre-mixing with linear polyions. *Chem Lett* 1997;26:25–6. <https://doi.org/10.1246/cl.1997.25>.
- [53] Lvov Y, Ariga K, Onda M, Ichinose I, Kunitake T. Alternate assembly of ordered multilayers of SiO<sub>2</sub> and other nanoparticles and polyions. *Langmuir* 1997;13:6195–202. <https://doi.org/10.1021/la970517x>.
- [54] Sun J, Wang L, Gao J, Wang Z. Control of composition in the multilayer films fabricated from mixed solutions containing two dendrimers. *J Colloid Interface Sci* 2005;287:207–12. <https://doi.org/10.1016/j.jcis.2005.01.068>.
- [55] Grant PS, McShane MJ. Development of multilayer fluorescent thin film chemical sensors using electrostatic self-assembly. *IEEE Sensors J* 2003;3:139–46. <https://doi.org/10.1109/JSEN.2002.807484>.
- [56] Guo Y, Geng W, Sun J. Layer-by-layer deposition of polyelectrolyte-polyelectrolyte complexes for multilayer film fabrication. *Langmuir* 2009;25:1004–10. <https://doi.org/10.1021/la803479a>.
- [57] vander Straeten A, Bratek-Skicki A, Germain L, D'Haese C, Eloy P, Fustin CA, et al. Protein-polyelectrolyte complexes to improve the biological activity of proteins in layer-by-layer assemblies. *Nanoscale* 2017;9:17186–92. <https://doi.org/10.1039/c7nr04345g>.
- [58] vander Straeten A, Dupont-Gillain C. Self-Reorganizing Multilayer to Release Free Proteins from Self-Assemblies. *Langmuir* 2020;36:972–8. <https://doi.org/10.1021/acslangmuir.9b03547>.
- [59] Ivanova K, Fernandes MM, Francesko A, Mendoza E, Guezguez J, Burnet M, et al. Quorum-Quenching and Matrix-Degrading Enzymes in Multilayer Coatings Synergistically Prevent Bacterial Biofilm Formation on Urinary Catheters. *ACS Appl Mater Interfaces* 2015;7:27066–77. <https://doi.org/10.1021/acscami.5b09489>.
- [60] Allais M, Meyer F, Ball V. Multilayered films made from tannic acid and alkaline phosphatase with enzymatic activity and electrochemical behavior. *J Colloid Interface Sci* 2018;512:722–9. <https://doi.org/10.1016/j.jcis.2017.10.101>.
- [61] Luo LL, Wang GX, Li YL, Yin TY, Jiang T, Ruan CG. Layer-by-layer assembly of chitosan and platelet monoclonal antibody to improve biocompatibility and release character of PLLA coated stent. *J Biomed Mater Res - Part A* 2011;97(A):423–32. <https://doi.org/10.1002/jbm.a.33066>.
- [62] Li R, Cui X, Hu W, Lu Z, Li CM. Fabrication of oriented poly-L-lysine/bacteriorhodopsin-embedded purple membrane multilayer structure for enhanced photoelectric response. *J Colloid Interface Sci* 2010;344:150–7. <https://doi.org/10.1016/j.jcis.2009.12.013>.
- [63] Caruso F, Fiedler H, Haage K. Assembly of  $\beta$ -glucosidase multilayers on spherical colloidal particles and their use as active catalysts. *Colloids Surfaces A Physicochem Eng Asp* 2000;169:287–93. [https://doi.org/10.1016/S0927-7757\(00\)00443-X](https://doi.org/10.1016/S0927-7757(00)00443-X).
- [64] Caruso F, Mohwald H. Protein multilayer formation on colloids through a stepwise self-assembly technique. *J Am Chem Soc* 1999;121:6039–46. <https://doi.org/10.1021/ja990441m>.
- [65] Zhou Z, Anselmo AC, Mitragotri S. Synthesis of protein-based, rod-shaped particles from spherical templates using layer-by-layer assembly. *Adv Mater* 2013;25:2723–7. <https://doi.org/10.1002/adma.201300220>.
- [66] Shah NJ, Macdonald ML, Beben YM, Padera RF, Samuel RE, Hammond PT. Tunable dual growth factor delivery from polyelectrolyte multilayer films. *Biomaterials* 2011;32:6183–93. <https://doi.org/10.1016/j.biomaterials.2011.04.036>.
- [67] Min J, Braatz RD, Hammond PT. Tunable staged release of therapeutics from layer-by-layer coatings with clay interlayer barrier. *Biomaterials* 2014;35:2507–17. <https://doi.org/10.1016/j.biomaterials.2013.12.009>.
- [68] Min J, Choi KY, Dreaden EC, Padera RF, Braatz RD, Spector M, et al. Designer Dual Therapy Nanolayered Implant Coatings Eradicate Biofilms and Accelerate Bone Tissue Repair. *ACS Nano* 2016;10:4441–50. <https://doi.org/10.1021/acsnano.6b00087>.
- [69] Macdonald ML, Samuel RE, Shah NJ, Padera RF, Beben YM, Hammond PT. Tissue integration of growth factor-eluting layer-by-layer polyelectrolyte multilayer coated implants. *Biomaterials* 2011;32:1446–53. <https://doi.org/10.1016/j.biomaterials.2010.10.052>.
- [70] Chen X, Luo J, Wu W, Tan H, Xu F, Li J. The influence of arrangement sequence on the glucose-responsive controlled release profiles of insulin-incorporated LbL films. *Acta Biomater* 2012;8:4380–8. <https://doi.org/10.1016/j.actbio.2012.08.014>.
- [71] Ram MK, Bertoncello P, Ding H, Paddeu S, Nicolini C. Cholesterol biosensors prepared by layer-by-layer technique. *Biosens Bioelectron* 2001;16:849–56. [https://doi.org/10.1016/S0956-5663\(01\)00208-1](https://doi.org/10.1016/S0956-5663(01)00208-1).
- [72] Shin YJ, Kameoka J. Amperometric cholesterol biosensor using layer-by-layer adsorption technique onto electrospun poly(amine) nanofibers. *J Ind Eng Chem* 2012;18:193–7. <https://doi.org/10.1016/j.jiec.2011.11.009>.
- [73] Moraes ML, de Souza NC, Hayasaka CO, Ferreira M, Rodrigues Filho UP, Riul A, et al. Immobilization of cholesterol oxidase in LbL films and detection of cholesterol using ac measurements. *Mater Sci Eng C* 2009;29:442–7. <https://doi.org/10.1016/j.msec.2008.08.040>.
- [74] Qin X, Wang H, Wang X, Li S, Miao Z, Huang N, et al. Amperometric choline biosensors based on multi-wall carbon nanotubes and layer-by-layer assembly of multilayer films composed of Poly(diallyldimethylammonium chloride) and choline oxidase. *Mater Sci Eng C* 2009;29:1453–7. <https://doi.org/10.1016/j.msec.2008.11.020>.
- [75] Shi H, Song Z, Huang J, Yang Y, Zhao Z, Anzai JI, et al. Effects of the type of polycation in the coating films prepared by a layer-by-layer deposition technique on the properties of amperometric choline sensors. *Sensors Actuators B Chem* 2005;109:341–7. <https://doi.org/10.1016/j.snb.2004.12.068>.
- [76] Sultana N, Schenkman JB, Rusling JF. Protein film electrochemistry of microsomes genetically enriched in human cytochrome P450 monooxygenases. *J Am Chem Soc* 2005;127:13460–1. <https://doi.org/10.1021/ja0538334>.
- [77] Chen D, Wu M, Chen J, Zhang C, Pan T, Zhang B, et al. Robust, flexible, and Bioadhesive free-standing films for the co-delivery of antibiotics and growth factors. *Langmuir* 2014;30:13898–906. <https://doi.org/10.1021/la503684k>.
- [78] Ma L, Zhou J, Gao C, Shen J. Incorporation of basic fibroblast growth factor by a layer-by-layer assembly technique to produce bioactive substrates. *J Biomed Mater Res - Part B Appl Biomater* 2007;83:285–92. <https://doi.org/10.1002/jbm.b.30794>.
- [79] Loew N, Scheller FW, Wollenberger U. Characterization of self-assembling of glucose dehydrogenase in mono- and multilayers on gold electrodes. *Electroanalysis* 2004;16:1149–54. <https://doi.org/10.1002/elan.200403005>.
- [80] Nickel A, Ohmann R, Meyer J, Grisolia M, Joachim C, Moresco F, et al. Moving nanostructures: Pulse-induced positioning of supramolecular assemblies. *ACS Nano* 2013;7:191–7. <https://doi.org/10.1021/nn303708h>.
- [81] Chen X, Wu W, Guo Z, Xin J, Li J. Controlled insulin release from glucose-sensitive self-assembled multilayer films based on 21-arm star polymer. *Biomaterials* 2011;32:1759–66. <https://doi.org/10.1016/j.biomaterials.2010.11.002>.
- [82] Suye SI, Zheng H, Okada H, Hori T. Assembly of alternating polymerized mediator, polymerized coenzyme, and enzyme modified electrode by layer-by-layer adsorption technique. *Sensors Actuators B Chem* 2005;108:671–5. <https://doi.org/10.1016/j.snb.2004.11.090>.
- [83] Caruso F, Schuler C. Enzyme multilayers on colloid particles: Assembly, stability, and enzymatic activity. *Langmuir* 2000;16:9595–603. <https://doi.org/10.1021/la000942h>.
- [84] Sun C, Li W, Sun Y, Zhang X, Shen J. Fabrication of multilayer films containing horseradish peroxidase based on electrostatic interaction and their application as a hydrogen peroxide sensor. *Electrochim Acta* 1999;44:3401–7. [https://doi.org/10.1016/S0013-4686\(99\)00059-6](https://doi.org/10.1016/S0013-4686(99)00059-6).
- [85] Yu X, Sotzing GA, Papadimitrakopoulos F, Rusling JF. Wiring of enzymes to electrodes by ultrathin conductive polyanion underlayers: Enhanced catalytic response to hydrogen peroxide. *Anal Chem* 2003;75:4565–71. <https://doi.org/10.1021/ac034188r>.
- [86] Narvez A, Suarez G, Popescu IC, Katakis I, Domnguez E. Reagentless biosensors based on self-deposited redox polyelectrolyte-oxidoreductases architectures. *Biosens Bioelectron* 2000;15:43–52. [https://doi.org/10.1016/S0956-5663\(00\)00049-X](https://doi.org/10.1016/S0956-5663(00)00049-X).
- [87] Brynda E, Houska M, Škvor J, Ramsden JJ. Immobilisation of multilayer bioreceptor assemblies on solid substrates. *Biosens Bioelectron* 1998;13:165–72. [https://doi.org/10.1016/S0956-5663\(97\)00107-3](https://doi.org/10.1016/S0956-5663(97)00107-3).
- [88] Zhang H, Yu Y, Cui S. Multilayer fluorescent thin films based on keratin-stabilized silver nanoparticles. *Colloids Surfaces A Physicochem Eng Asp* 2011;384:501–6. <https://doi.org/10.1016/j.colsurfa.2011.05.025>.
- [89] Sirkar K, Revzin A, Pishko MV. Glucose and lactate biosensors based on redox polymer/oxidoreductase nanocomposite thin films. *Anal Chem* 2000;72:2930–6. <https://doi.org/10.1021/ac991041k>.
- [90] Szamocki R, Flexer V, Levin L, Forchiasin F, Calvo EJ. Oxygen cathode based on a layer-by-layer self-assembled laccase and osmium redox mediator. *Electrochim Acta* 2009;54:1970–7. <https://doi.org/10.1016/j.electacta.2008.09.002>.
- [91] Xing Q, Eadula SR, Lvov YM. Cellulose fiber-enzyme composites fabricated through layer-by-layer nanoassembly. *Biomacromolecules* 2007;8:1987–91. <https://doi.org/10.1021/bm070125x>.
- [92] Patel DS, Aithal RK, Krishna G, Lvov YM, Tien M, Kuila D. Nano-assembly of manganese peroxidase and lignin peroxidase from *P. chrysosporium* for biocatalysis in aqueous and non-aqueous media. *Colloids Surf B: Biointerfaces* 2005;43:13–9. <https://doi.org/10.1016/j.colsurfb.2005.03.007>.

- [93] Baek H, Lee C, Lim K II, Cho J Resistive switching memory properties of layer-by-layer assembled enzyme multilayers *Nanotechnology* 2012;23:155604. <https://doi.org/10.1088/0957-4484/23/15/155604>.
- [94] Constantine CA, Mello SV, Dupont A, Cao X, Santos D, Oliveira ON, et al. Layer-by-layer self-assembled chitosan/poly(thiophene-3-acetic acid) and organophosphorus hydrolase multilayers. *J Am Chem Soc* 2003;125:1805–9. <https://doi.org/10.1021/ja028691h>.
- [95] Constantine CA, Gattás-Asfura KM, Mello SV, Crespo G, Rastogi V, Cheng TC, et al. Layer-by-Layer Films of Chitosan, Organophosphorus Hydrolase and Thioglycolic Acid-Capped CdSe Quantum Dots for the Detection of Paraoxon. *J Phys Chem B* 2003;107:13762–4. <https://doi.org/10.1021/jp036381v>.
- [96] Hong J, Kim BS, Char K, Hammond PT. Inherent charge-shifting polyelectrolyte multilayer blends: A facile route for tunable protein release from surfaces. *Biomacromolecules* 2011;12:2975–81. <https://doi.org/10.1021/bm200566k>.
- [97] Forzani ES, Solís VM, Calvo EJ. Electrochemical behavior of polyphenol oxidase immobilized in self-assembled structures layer by layer with cationic polyallylamine. *Anal Chem* 2000;72:5300–7. <https://doi.org/10.1021/ac0003798>.
- [98] Coche-Guérente L, Desbrières J, Fatisson J, Labbé P, Rodriguez MC, Rivas G. Physicochemical characterization of the layer-by-layer self-assembly of polyphenol oxidase and chitosan on glassy carbon electrode. *Electrochim Acta* 2005;50:2865–77. <https://doi.org/10.1016/j.electacta.2004.11.040>.
- [99] Coche-Guerente L, Labbé P, Menges V. Amplification of amperometric biosensor responses by electrochemical substrate recycling. 3. Theoretical and experimental study of the phenol-polyphenol oxidase system immobilized in laponite hydrogels and layer-by-layer self-assembled structures. *Anal Chem* 2001;73:3206–18. <https://doi.org/10.1021/ac001534i>.
- [100] Garbers E, Mitlöchner R, Georgieva R, Bäumler H. Activity of immobilized trypsin in the layer structure of polyelectrolyte microcapsules (PEMC). *Macromol Biosci* 2007;7:1243–9. <https://doi.org/10.1002/mabi.200700117>.
- [101] Hoshi T, Saiki H, Anzai JI. Amperometric uric acid sensors based on polyelectrolyte multilayer films. *Talanta* 2003;61:363–8. [https://doi.org/10.1016/S0039-9140\(03\)00303-5](https://doi.org/10.1016/S0039-9140(03)00303-5).
- [102] Wang HG, Yin TY, Ge SP, Zhang Q, Dong QL, Lei DX, et al. Biofunctionalization of titanium surface with multilayer films modified by heparin-VEGF-fibronectin complex to improve endothelial cell proliferation and blood compatibility. *J Biomed Mater Res - Part A* 2013;101(A):413–20. <https://doi.org/10.1002/jbm.a.34339>.
- [103] Caldwell JW, Arsuru EL, Kilgore WB, Garcia AL, Reddy V, Johnson RH. Layer-by-layer assembly of collagen thin films: Controlled thickness and biocompatibility. *Biomed Microdevices* 2001;3:301–6. <https://doi.org/10.1023/A:1012456714628>.
- [104] Landoulsi J, Demoustier-Champagne S, Dupont-Gillain C. Self-assembled multilayers based on native or denatured collagen: Mechanism and synthesis of size-controlled nanotubes. *Soft Matter* 2011;7:3337–47. <https://doi.org/10.1039/c0sm00918k>.
- [105] Johansson JÅ, Halthur T, Herranen M, Söderberg L, Elofsson U, Hillborn J. Build-up of collagen and hyaluronic acid polyelectrolyte multilayers. *Biomacromolecules* 2005;6:1353–9. <https://doi.org/10.1021/bm0493741>.
- [106] Fujie T, Furutate S, Niwa D, Takeoka S. A nano-fibrous assembly of collagen-hyaluronic acid for controlling cell-adhesive properties. *Soft Matter* 2010;6:4672–6. <https://doi.org/10.1039/c0sm00527d>.
- [107] Chen J, Chen C, Chen Z, Chen J, Li Q, Huang N. Collagen/heparin coating on titanium surface improves the biocompatibility of titanium applied as a blood-contacting biomaterial. *J Biomed Mater Res - Part A* 2010;95(A):341–9. <https://doi.org/10.1002/jbm.a.32847>.
- [108] Cool SM, Kenny B, Wu A, Nurcombe V, Trau M, Cassady AI, et al. Poly(3-hydroxybutyrate-co-3-hydroxyvalerate) composite biomaterials for bone tissue regeneration: In vitro performance assessed by osteoblast proliferation, osteoclast adhesion and resorption, and macrophage proinflammatory response. *J Biomed Mater Res - Part A* 2007;82:599–610. <https://doi.org/10.1002/jbm.a.31174>.
- [109] Lin Q, Ding X, Qiu F, Song X, Fu C, Ji J. In situ endothelialization of intravascular stents coated with an anti-CD34 antibody functionalized heparin-collagen multilayer. *Biomaterials* 2010;31:4017–25. <https://doi.org/10.1016/j.biomaterials.2010.01.092>.
- [110] Chen JL, Li QL, Chen JY, Chen C, Huang N. Improving blood-compatibility of titanium by coating collagen-heparin multilayers. *Appl Surf Sci* 2009;255:6894–900. <https://doi.org/10.1016/j.apsusc.2009.03.011>.
- [111] Nawae S, Meesane J, Muensit N, Daengngam C. Layer-by-layer self-assembled films of silk fibroin/collagen/poly (diallyldimethylammonium chloride) as nucleating surface for osseointegration to design coated dental implant materials. *Mater Des* 2018;160:1158–67. <https://doi.org/10.1016/j.matdes.2018.10.041>.
- [112] He W, Bellamkonda RV. Nanoscale neuro-integrative coatings for neural implants. *Biomaterials* 2005;26:2983–90. <https://doi.org/10.1016/j.biomaterials.2004.08.021>.